รายงานวิจัยฉบับสมบูรณ์

โครงการ

การวิเคราะห์ความหลากหลายของยีน alcohol dehydrogenase (*adh*) และกลไกการทนกรดน้ำส้ม และเอทานอลในแบคทีเรียกรดน้ำส้ม

โดย

นางสาวปิยวรรณ ชิณณะวิโรจน์ไพศาล

ผศ. ดร. กัญจนา ธีระกุล

ภาควิชาจุลชีววิทยา คณะวิทยาศาสตร์

มหาวิทยาลัยเกษตรศาสตร์

19 กันยายน 2546

สัญญาเลขที่ BGJ/09/2544

รายงานวิจัยฉบับสมบูรณ์

โครงการ
การวิเคราะห์ความหลากหลายของยีน alcohol dehydrogenase (*adh*) และกลไกการทนกรดน้ำส้ม และเอทานอลในแบคทีเรียกรดน้ำส้ม

โดย
นางสาวปิยวรรณ ชิณณะวิโรจน์ไพศาล
ผศ. ดร. กัญจนา ธีระกุล

ภาควิชาจุลชีววิทยา คณะวิทยาศาสตร์
มหาวิทยาลัยเกษตรศาสตร์

สนับสนุนโดยสำนักงานกองทุนสนับสนุนการวิจัย

ABSTRACT

Project code: BGJ/49/003

Project Title: Analysis of Variation in Alcohol Dehydrogenase Gene and Mechanism of Tolerance to Acetic Acid and Ethanol in Acetic Acid Bacteria

Investigators: Ms. Piyawan Chinnawirotpisan, Ph.D. student

Assist. Prof. Dr. Gunjana Theeragool, Kasetsart University

E-mail Address: fscgmt@ku.ac.th

Project Period: 2 years (May 1, 2001 – May 1, 2003)

The relationship between quinoprotein alcohol dehydrogenase (PQQ-ADH) and NAD-dependent alcohol dehydrogenase (NAD-ADH) was studied by construction of quinoprotein ADH-deficient mutants. The quinoprotein ADH-deficient mutants were successfully constructed from *Acetobacter pasteurianus* SKU1108 by NTG mutagenesis and adhA gene disruption with kanamycin cassette. The PQQ-ADH-deficient mutant (NTG mutant CN6-2) exhibited a complete loss in ethanol-oxidizing ability and acetic acid resistance, while the ADH-disruptant DP3 exhibited a complete loss in acetic acid resistance but retained weak ADH activity. The NTG mutant CN6-2 grew even better than the wild strain in ethanol-containing medium despite of no ability to oxidize ethanol. In addition, two NAD-dependent ADHs (ADH I and ADH II), present in a small amount in the wild strain, were increased dramatically in the cytoplasm of NTG mutant when cultured in the medium containing ethanol, concomitant to the increase of the key enzyme activities in TCA and glyoxylate cycles. Whereas, the disruptant DP3 grew lower than the wild strain, producing lower amount of acetic acid in the ethanol culture, and induced one of two NAD-ADHs (ADH I) and some of the acetate-assimilating enzymes induced in the NTG mutant. Two inducible NAD-ADHs were purified and characterized from the soluble fraction of the NTG mutant. One (ADH I) is a trimer, consisting of three identical subunits of 42 kDa, while the other (ADH II) is a homodimer, having two subunits of 31 kDa. The two NAD-ADHs showed clear difference in their kinetics and substrate specificity. This study clearly showed that PQQ-ADH is extensively involved in acetic acid production, while NAD-ADHs only for ethanol assimilation through the TCA and glyoxylate cycles, in acetic acid bacteria.

Keywords: acetic acid bacteria, alcohol dehydrogenase, ethanol tolerance, acetic acid resistance

บทคัดย่อ

รหัสโครงการ BIG4485009

ชื่อโครงการ การวิเคราะห์ความหลากหลายของยีน alcohol dehydrogenase (adh) และกลไกการทนกรดน้ำส้มและเอทานอลในแบคทีเรียกรดน้ำส้ม

ชื่อนักวิจัยและสถาบัน นางสาวปิยะรวรรณ ขันณะวิโรจน์ไพศาล นิสิตปริญญาเอก

ผศ. ดร. กัญจนา ธีระกุล มหาวิทยาลัยเกษตรศาสตร์

E-mail Address : fscignt@ku.ac.th

ระยะเวลาโครงการ 2 ปี (1 พฤษภาคม 2544 ถึง 1 พฤษภาคม 2546)

การศึกษาความสัมพันธ์ระหว่างเอนไซม์ quinoprotein แอลกอฮอล์ดีไฮโดรจีเนส (PQQ-ADH) และ NAD-dependent แอลกอฮอล์ดีไฮโดรจีเนส (NAD-ADH) ทำโดยการสร้างสายพันธุ์กลายที่ขาดกิจกรรมของเอนไซม์ quinoprotein แอลกอฮอล์ดีไฮโดรจีเนส โดยการเหนี่ยวนำให้เกิดการกลายพันธุ์โดยใช้สารเคมี NTG และการ disrupt ยีน adhA ด้วยยีน kanamycin สายพันธุ์กลาย CN5-2 ที่ได้จาก NTG ขาดความสามารถในการผลิตและการทนต่อกรดน้ำส้มอย่างสมบูรณ์ ในขณะที่ ADH-disruptant DP3 ขาดความสามารถในการทนต่อกรดน้ำส้มอย่างสมบูรณ์แต่ยังมีกิจกรรมของเอนไซม์ quinoprotein แอลกอฮอล์ดีไฮโดรจีเนสบางส่วน ในสายพันธุ์กลาย NTG พบว่ากิจกรรมของเอนไซม์ NAD-dependent แอลกอฮอล์ดีไฮโดรจีเนส (ADH I และ ADH II) ที่พบในปริมาณน้อยมากในสายพันธุ์พ่อแม่กลับเพิ่มขึ้นอย่างเห็นได้ชัดเมื่อเลี้ยงในอาหารที่เติมเอทานอล ควบคู่กับการเพิ่มขึ้นของกิจกรรมของเอนไซม์หลัก ใน TCA และ glyoxylate cycles ในขณะที่ ADH-disruptant DP3 เจริญช้ากว่าสายพันธุ์เดิม ผลิตกรดน้ำส้มได้เล็กน้อย ถูกเหนี่ยวให้สร้าง NAD-dependent แอลกอฮอล์ดีไฮโดรจีเนส เฉพาะ ADH I และเอนไซม์ที่เกี่ยวข้องกับการใช้ acetate บางชนิดที่ถูกเหนี่ยวให้สร้างในสายพันธุ์กลาย NTG จากการแยกบริสุทธิ์และศึกษาคุณสมบัติของ NAD-dependent แอลกอฮอล์ดีไฮโดรจีเนส 2 ชนิด พบว่า ADH I เป็น trimer ประกอบด้วยหน่วยย่อยที่เหมือนกัน 3 หน่วย แต่ละหน่วยมีขนาด 42 กิโลดาลตัน ส่วน ADH II เป็น dimer ประกอบด้วยหน่วยย่อยที่เหมือนกัน 2 หน่วย แต่ละหน่วยมีขนาด 31 กิโลดาลตัน เอนไซม์ทั้งสองนี้แสดงความแตกต่างของค่าจลนศาสตร์และความจำเพาะต่อสารตั้งต้นอย่างเด่นชัด จากการศึกษาทั้งหมดนี้แสดงให้เห็นอย่างชัดเจนว่าเอนไซม์ quinoprotein แอลกอฮอล์ดีไฮโดรจีเนสทำหน้าที่เกี่ยวกับการผลิตกรดน้ำส้ม ในขณะที่เอนไซม์ NAD-dependent แอลกอฮอล์ดีไฮโดรจีเนสมีบทบาทเกี่ยวกับการใช้ เอทานอลผ่าน TCA และ glyoxylate cycles ในแบคทีเรียกรดน้ำส้ม

คำหลัก แบคทีเรียกรดน้ำส้ม, แอลกอฮอล์ดีไฮโดรจีเนส, การทนเอทานอล, การทนกรดน้ำส้ม

กิตติกรรมประกาศ

คณะผู้วิจัย ขอขอบคุณสำนักงานกองทุนสนับสนุนการวิจัย (สกว.) ที่ให้การสนับสนุนทุนวิจัยองค์ความรู้ใหม่ในการสร้างนักวิจัยระดับปริญญาเอก กลุ่ม ... และทุนโครงการปริญญาเอกกาญจนาภิเษก ภาควิชาชีวเคมี คณะวิทยาศาสตร์ มหาวิทยาลัยเกษตรศาสตร์ และ Department of Biological Chemistry, Faculty of Agriculture, Yamaguchi University ที่สนับสนุนสถานที่ เครื่องมือ อุปกรณ์ และสารเคมีในการทำวิจัย Association of International Education, Japan (AIEJ) ที่สนับสนุนค่าเดินทางและค่าครองชีพในระหว่างเข้าร่วมการประชุม ชัณณะวิโรจน์ไพศาล ทำวิจัยที่ประเทศญี่ปุ่น Japan Society for Promotion of Science (JSPS) ที่สนับสนุนค่าเดินทางและค่าครองชีพในการเดินทางไปทำวิจัยที่ประเทศญี่ปุ่น และ ศ. ดร. กัญจนา ฮิระกุล และ National Research Council of Thailand (NRCT) ที่ให้การสนับสนุนความร่วมมือทางวิชาการกับ JSPS.

นางสาวปิยะรวม ชัณณะวิโรจน์ไพศาล

ผศ. ดร. กัญจนา ฮิระกุล

กันยายน 2546

INTRODUCTION

Acetic acid bacteria are obligate aerobic bacteria belonging to α-Proteobacteria, and divided into six genera namely, *Acetobacter*, *Gluconobacter*, *Gluconacetobacter*, *Asa*, *Acidomonas* and *Kozaka* (Lisdiyanti et al., 2000; 2001; 2002; Yamada et al., 1999; Yamada, 2000). *Acetobacter* species and also *Gluconacetobacter* are well known as vinegar producers for more than 100 years ago. Nevertheless, it was believed that acetic acid was produced by the actions of cytosolic NAD(P)-dependent alcohol dehydrogenase. Thereafter, it has been fixed that acetic acid bacteria produce acetic acid from ethanol by two sequential oxidation reactions of membrane-bound alcohol dehydrogenase (ADH) and aldehyde dehydrogenase (ALDH), localized on the periplasmic side of the cytoplasmic membrane (Matsushita et al., 1994). The membrane-bound ADH has been shown to have pyrroloquinoline quinone (PQQ) as the prosthetic group. PQQ-dependent ADH has been found in several other aerobic bacteria such as *Pseudomonas*, *Comamonas*, or *Ralstonia* species. Among such quinoprotein ADHs, ADH in acetic acid bacteria is rather unique because of consisting of three different subunits. It contains additional prosthetic groups for multiple heme c, and being present in the membrane, and thus termed as type III quinoprotein ADH, distinguished from other soluble type I and type II ADHs. Type I ADH is a quinoprotein having PQQ as only prosthetic group, while type II ADH is a quinohemoprotein having a heme c beside PQQ. Whereas, type III ADH of acetic acid bacteria is a quinohemoprotein-cytochrome c complex, where the largest subunit (subunit I) is a quinohemoprotein, the second subunit (subunit II) contains three heme c motifs in the molecule, and the smallest subunit (subunit III) is suggested to work as a molecular chaperon of subunit I.

Acetic acid bacteria also have an additional ADH, which is more general NAD(P)-dependent enzyme, in the cytoplasm at lower level. NAD(P)-dependent ADHs can be divided into three groups according to their structures (Jornvall et al., 1987). Group I is a zinc-dependent, long-chain ADH family. Group II is a zinc-independent, short-chain ADH family. Group III is an "iron activated" ADHs. Many organisms have been reported to contain multiple NAD-dependent ADHs, the physiological roles of which have sometimes been proven to be difficult to disentangle (Ismail et al., 1993). In acetic acid bacteria, ethanol is oxidized extensively by the membrane-bound quinoprotein ADH and only low NAD-dependent ADH activity is detected in the cytoplasm (Matsushita et al., 1994).

Recently, a thermotolerant strain, *Acetobacter pasteurianus* SKU1108 (re-identified) based on 16S rDNA sequences, was isolated from pineapple in Thailand. This strain produced high amount of acetic acid and also possesses high tolerance to acetic acid even at higher temperature (Saeki *et al.*, 1997a). Such ethanol oxidation and acetic acid resistance have been suggested to be deeply related each other, and to be related to quinoprotein ADH. In this work, in order to elucidate the functions of quinoprotein ADH, quinoprotein ADH-deficient mutants were derived from *A. pasteurianus* SKU1108 by *N*-methyl-*N*'-nitro-*N*-nitrosoguanidine (NTG) mutagenesis and *adhA* gene disruption. Then the NTG mutant and the ADH-disruptant were characterized comparing with the wild-type strain. During the analysis of the NTG mutant, it was found that the mutant strain grows even better than wild-type strain, despite of no ability to oxidize ethanol, and that two NAD-dependent ADHs, present in a small amount in the wild-type strain, are increased dramatically in the cytoplasm when cultured in the medium containing ethanol. There has been no report on NAD-dependent ADHs in acetic acid bacteria so far. Therefore, the purification and characterization of two NAD-dependent ADHs from the soluble fraction of the NTG mutant were carried out. Characterization of the two ADHs indicated that one (ADH I) is a member of the long-chain family and shows a preference for primary alcohols and another (ADH II) is a member of the short-chain family shows a preference for secondary alcohols (Chinnawirotpisan *et al.*, 2003a). Moreover, it was shown that defect in quinoprotein ADH I leads a global metabolic change from ethanol oxidation to ethanol assimilation, which is accompanied with the induction of two different NAD-dependent ADHs. This study indicates conclusively that membrane-bound quinoprotein ADH is extensively involved in acetic acid production, while NAD-dependent ADH only for ethanol assimilation, in acetic acid bacteria (Chinnawirotpisan *et al.*, 2003b).

OBJECTIVES

1. To purify and characterize quinoprotein alcohol dehydrogenase (PQQ-ADH) and two inducible NAD-dependent alcohol dehydrogenases in *A. pasteurianus* SKU1108 and its PQQ-ADH deficient mutants.
2. To study the roles of quinoprotein and NAD-dependent alcohol dehydrogenases (NAD-ADHs) in *A. pasteurianus* SKU1108 and its PQQ-ADH deficient mutants.

MATERIALS AND METHODS

1. Bacterial strains, culture medium, and culture conditions

A thermotolerant *Acetobacter pasteurianus* SKU1108 was previously isolated from pineapple in Thailand (Theeragool et al., 1996). The quinoprotein ADH-deficient mutants were constructed in *A. pasteurianus* SKU1108. The NTG mutant CN6-2 was obtained from the culture stock (Jakeawatana, 2001, personal communication), while the ADH-disruptant DP3 was constructed in this study. Two different culture media were used in this study according to the purpose of individual experiments; potato medium containing 0.5% $CaCO_3$ and 1.5% agar was used for stock cultures, and YPGD medium was for the study of bacterial growth and enzyme activity measurements. Ethanol was added aseptically when indicated. Five ml of an overnight culture in the potato medium was inoculated to 100 ml of YPGD medium in 500 ml Erlenmeyer flask with a side-arm. Cultivation was done at 30°C on a rotary shaker at 200 rpm. The growth was measured with a Klett Summerson photometer periodically through the side arm without the cotton stopper being removed.

Escherichia coli DH5α was used as host cell for gene cloning and routinely cultured in Luria Bertani broth. Ampicillin and kanamycin were added to the medium at a final concentration of 50 μg/ml and tetracycline was also used at a final concentration of 25 μg/ml when necessary to maintain plasmids.

For membrane-bound quinoprotein ADH purification, *A. pasteurianus* SKU1108 wild-type strain was inoculated into 5 ml of the potato medium and incubated for 18 h at 30°C with shaking at 200 rpm. The seed culture was prepared as described above. The seed culture was transferred to 1 liter of YPGD medium containing 4% ethanol and cultivated for 48 h.

For soluble NAD-dependent ADH purification, *A. pasteurianus* CN6-2 was inoculated into 5 ml of the potato medium and incubated for 18 h at 30°C with shaking at 200 rpm. The seed culture was transferred to 100 ml of the same medium in a 500 ml Erlenmeyer flask and cultivated for 24 h. The seed culture was transferred to 1 liter of YPGD medium, in which 4% ethanol (v/v) was added aseptically, in a 3 liter Erlenmeyer flask, and cultivated for 48 h.

2. Preparation of cell-free extract

All operations were done at 4°C unless state otherwise. Bacterial cells were harvested by centrifugation at 9,000 rpm for 10 min, and washed twice with ice-cold 50 mM potassium

phosphate buffer (KPB), pH 7.5, containing 1 mM dithiothreitol (DTT) and 1 mM $MgCl_2$. The washed cells were resuspended at about 1 g of wet cells per 4 ml in the same buffer and passed twice through a French pressure cell press (American Instruments, Co., Silver Spring, MD., USA) at 16,000 psi. Cell debris was removed by centrifugation at 9,000 rpm for 10 min, the supernatant was centrifuged at 40,000 rpm for 90 min to separate soluble fraction from membrane fraction. The resulting supernatant was used for further purification of NAD-dependent enzymes. For enzyme activity measurement, the soluble fraction was dialyzed overnight with the same buffer. The dialyzed solution was spun down to remove insoluble materials and the supernatant was used as cytoplasm. The membrane fraction was homogenized with 10 mM KPB (pH 6.0) and used as the membrane. For membrane bound quinoprotein ADH purification, cells were harvested as described above. The cell paste was suspended in 50 mM KPB (pH 6.0) about 1 g of wet cells per 4 ml of buffer, and passed through a French pressure cell press as mentioned above. The obtained membrane fraction was used for further purification.

3. Purification and characterization of membrane-bound quinoprotein alcohol dehydrogenase (PQQ-ADH)

All operations were done at 4°C. The membrane fraction of thermotolerant *A. paslteurianus* SKU1108 wild type strain was suspended to a final protein concentration of about 10 mg/ml in 10 mM KPB (pH 6.0), and Triton X-100 was added to the final concentration of 1%. The membrane suspension was stirred gently on ice for 90 min and ultracentrifugation at 40,000 rpm for 1 h. The resulting supernatant was then dialyzed overnight against 5 mM KPB (pH 6.0) containing 0.1% Triton X-100. The dialysate was applied onto a DEAE-Toyopearl column (about 1 ml of bed volume per 3 mg of protein), which had been equilibrated with the same buffer. After the column was washed with 3 bed volumes of the same buffer, the enzyme was eluted by a concave-type gradient system in the presence of 0.1% Triton X-100. The gradient was made up with two-buffer systems consisting of 4 bed volumes of 5 mM KPB (pH 6.0) and 2 bed volumes of 50 mM KPB (pH 6.0), in which both buffers contained 0.1% Triton X-100. The active fraction from a DEAE-Toyopearl column was collected and dialyzed against 50 mM KPB (pH 6.0) containing 0.1% Triton X-100. The combined active fraction of membrane-bound ADH was dialyzed with 50 mM KPB (pH 6.0). The dialyzed sample was applied onto a hydroxyl apatite

(about 1 ml of bed volume per 3 mg of protein) which had been equilibrated with the same buffer. The column was washed with 3 bed volumes of the same buffer, the enzyme was eluted by stepwise with 100 and 150 mM KPB (pH 6.0) containing 0.1% Triton X-100. The whole enzyme activity was eluted with 150 mM KPB (pH 6.0). The combined active fraction was concentrated by ultrafiltration with a UP20 membrane (Advantec Toyo). The concentrated enzyme was used for further analysis of acetic acid resistance.

The purity and molecular mass of the purified enzyme was analyzed by SDS-PAGE. After electrophoresis, the proteins were stained with Coomassie brilliant blue R-250. Heme staining was done with heme-catalyzed peroxidase activity. The pre-stained protein marker (BioRad) was used as markers for estimation of relative mobility. Effect of acetic acid against ADH activity was done in 10 mM KPB (pH 6.0) containing various concentration of acetic acid by using membrane fraction and purified enzyme. Effect of sodium acetate and pH against ADH activity were also determined.

4. Purification and characterization of two inducible NAD-dependent alcohol dehydrogenases (NAD-ADHs)

All steps were done at 4°C. KPB (pH7.5) of various concentrations containing 1 mM DTT and 1 mM $MgCl_2$ was used. The resulting supernatant after ultracentrifugation of *A. pasteurianus* CN8-2 NTG mutant was put directly on a DEAE-Toyopearl column (about 1 ml of bed volume per 3 mg of protein), which had been equilibrated with 50 mM KPB (pH 7.5). Under these conditions, most of the enzyme activity was not absorbed onto the column. The combined pass-through fraction having the enzyme activity was dialyzed with 5 mM KPB (pH 7.5), and put on an alternative column of DEAE-Toyopearl, which had been equilibrated with the same buffer. The column was washed with the column buffer and then eluted by a linear gradient of 5 to 50 mM KPB (pH 7.5). NAD-dependent ADH activity was separated into two fractions. One, with an activity preference for primary alcohols (ADH I), was eluted at 35 mM KPB (pH 7.5), while another enzyme activity having a preference for secondary alcohols (ADH II) was not adsorbed to the column. The two NAD-dependent ADH activity fractions were combined separately.

The combined active fraction of ADH I was dialyzed with 5 mM KPB (pH 7.5). The dialysate was put on a hydroxyl apatite column (about 3 ml of bed volume per 3 mg of protein), which had been equilibrated with the same buffer. The column was washed with the column

buffer and then eluted stepwise with 50, 100, and 500 mM KPB (pH 7.5). Almost all of the enzyme activity was eluted with 100 mM KPB (pH 7.5). The combined active fraction was concentrated by ultrafiltration with a UP20 membrane (Advantec Toyo). The concentrated enzyme (~1.5 ml) was dialyzed with 10 mM KPB (pH 7.5), and put on a DEAE-Toyopearl column which had been equilibrated with the same buffer. After washing the column with the column buffer, the enzyme was eluted with a linear gradient of 10 to 40 mM KPB (pH 7.5).

The combined active fraction of ADH II in the second DEAE-Toyopearl column was directly applied on a hydroxyl apatite column, which had been equilibrated with 5 mM KPB (pH 7.5). After the column was washed with the same buffer, the enzyme was eluted stepwise with 50, 100, and 500 mM KPB (pH 7.5). The whole enzyme activity was eluted with 100 mM KPB (pH 7.5). The combined active fraction was concentrated by ultrafiltration with a UP20 membrane (Advantec Toyo). One and half ml of the concentrated enzyme was put on a Superdex S-200 column, which had been equilibrated with 50 mM KPB (pH 7.5). The obtained enzyme from the final step was used for further analysis of kinetic parameters.

The purity and molecular mass of the purified enzymes were analyzed by SDS-PAGE as described by Laemmli et al., 1970. Before application, samples were mixed with 0.33 volume of 4 sample buffer and heated at 60°C for 30 min. Then, the treated samples were put on a 10% SDS-PAGE slab gel. For N-terminal amino acid sequencing, the separated proteins in SDS-PAGE were transferred electrophoretically onto PVDF membrane. Then, the membrane was stained with 0.1% Coomassie brilliant blue R-250 for 1 min, and destained with 50% methanol. The visible band was excised and put into a peptide sequence analyzer PSQ-2 (Shimadzu). The protein content was measured by the modified Lowry method. The relative molecular mass of the native enzyme were measured by gel filtration by using a Superdex S-200 column equilibrated with 50 mM KPB (pH 7.5) containing 1 mM DTT. The standard marker proteins used was obtained from Oriental Yeast, Co., Ltd., consisting of glutamate dehydrogenase (290,000 daltons), lactate dehydrogenase (142,000 daltons), enolase (67,000 daltons), myokinase (32,000 daltons), and cytochrome c (12,400 daltons). The metal content of the purified enzymes were measured by induced-coupled plasma atomic emission spectrometry (ICP-AES) using the internal standard method with Zn^{2+}, Mg^{2+}, and Fe^{2+}.

5. Characterization of quinoprotein alcohol dehydrogenase-deficient mutants (PQQ-ADH-deficient mutants)

Acidity of the culture medium was measured by titration with 0.5 N NaOH with phenolphthalein as the pH indicator and expressed as acetate concentration. Ethanol concentration in the culture medium was measured enzymatically (Ameyama, 1982), based on ferricyanide-dichloral method. The concentration of ethanol was determined by calculating with a standard curve.

5.1 16S ribosomal DNA sequencing and analysis Primers for the *in vitro* PCR amplification of 16S rDNA were kindly donated by Assoc. Prof. Dr. Kazuhei Yokoyama at the Department of Biological Chemistry, Faculty of Agriculture, Yamaguchi University. The primers were selected from highly conserved regions of bacterial rDNA genes. The 5' end (27f, 5'-AGAGTTTGATCCTGGCTCAG-3') and the 3' end (1524r, 5'-AAAGGAGGTGATCCAGCC-3') primers were used as described by Devereux and Wills, 1995.

PCR amplification was performed by using PCR Kit (Ready-To-Go™ PCR Beads) of Amersham Pharmacia Biotech, Inc., USA. DNA template (50 ng) and 100 pmol each of primers were added into PCR bead in 0.2 ml tube containing each deoxynucleotide triphosphate (dNTPs; dATP, dTTP, dCTP and dGTP) at a final concentration of 200 μmol, 1.5 mM $MgCl_2$, 10 mM Tris-HCl (pH 9.0), 50 mM KCl, and 1.5 unit of *Taq* DNA polymerase, and the final volume was adjusted to 25 μl with sterile distilled water. DNA amplification was performed with a model 2400 thermal cycler (Perkin-Elmer, Norwalk, Conn.) by using the following program: a 5 min hot start at 94 °C, following by 35 cycles consisting of denaturation (1 min at 94 °C), annealing (1 min at 50 °C), and extension (2 min at 72 °C) and a final extension at 72 °C for 10 min. The 1.5 kb PCR products were electrophoresis in a 0.8% agarose gel in TBE buffer at 50 volts. The PCR products were recovered from the gel by using QIAquick PCR Purification Kit. The nucleotide sequencing of the cloned 16S rDNA fragment was determined by applying the chain termination method using an ABI PRISM 310 genetic analyzer (PE Biosystms, Japan). All procedures were followed according to the manufacturer's instructions. DNA sequences were processed with GENETYXMAC, version 10.1 (Software development Co., Tokyo, Japan) for multi-alignment analysis.

5.2 Construction of the *adhA* gene disruptant. PCR was performed with chromosomal DNA of SKU1108 wild-type strain as a template by using the following oligonucleotide primers: 5'-end primer containing *Pst*I site (Primer A: 5'-GGTGTCTG CAGTTAACACCATCGC-3') and 3'-end primer containing *Sal*I site (Primer B: 5'-TGGCAAGCCACACAGTCGACTAGG-3') were designed to cover from 1,096 nt to 3,001 nt of adh4 gene of *A. pasteurianus* SKU1108. PCR amplification was performed by using PCR Kit with a DNA template (50 ng) and 20 pmol each of primers, and the final volume was adjusted to 25 µl with sterile distilled water. The PCR condition consists of a 5 min hot start at 95°C, following by 40 cycles of denaturation (30 sec at 95°C), annealing (30 sec at 55°C), and extension (3 min at 72°C) and a final extension at 72°C for 5 min. The obtained PCR products were electrophoresis in a 0.8% agarose gel in TBE buffer at 50 volts. The PCR products were recovered from the gel by using QIAquick PCR Purification Kit. The purified double-stranded PCR products were confirmed by agarose gel electrophoresis before used. The obtained PCR product, 1.9 kb DNA fragment, was introduced into pGEM-T Easy Vector System. The *Pst*I digested *adh* fragment was isolated from the above plasmid (one of the *Pst*I site is present in the T vector) and inserted into *Pst*I site on the ampicillin gene in pSUP202 (Simon *et al.*, 1983), to generate pSUP202 adh. The 1.2 kb *Bam*HI fragment carrying kanamycin cassette (Vieira and Messing, 1982) was inserted into *Bam*HI site in pSUP202 adh to generate pSUP202 adh::Km. The recombinant plasmid pSUP202 adh::Km was digested by *Eco*RV (188 nt on pSUP202) and the linearized adh fragment was introduced into *A. pasteurianus* SKU1108 by gene pulse II at 2.0 kV (resistance 200 ohms, capacitance 25 µF) as described by Mostafa *et al.*, 2003. The ADH-disruptants were selected on YPG medium containing 50 µg/ml of kanamycin, 0.8% $CaCO_3$, and 2% ethanol. Colonies deficient in ethanol-oxidizing ability were screened by the absence of clear zone. The selected quinoprotein ADH-deficient mutants were confirmed by using PCR amplification as described above.

5.3 Nucleotide sequencing of *adhA* gene and reverse transcriptase (RT) PCR. Total DNA of the wild-type and NTG mutant strains were prepared as described previously. PCR amplification were performed by using PCR Kit with a specific primers, 5'-end (Primer C: 5'-GGTGGGACCGTATGGGATYC-3') and 3'-end (Primer D: 5'-CCGCGACCAACCATTG-3'), which were selected from highly conserved regions of *adhA* gene (subunit I). DNA template (50 ng) and 20 pmol each of primers were added into PCR beads and the final volume was adjusted to

25 µl with sterile distilled water. DNA amplification was performed as follows: a hot start at 95°C for 5 min, following by 30 cycles consisting of denaturation (1 min at 95°C), annealing (2 min at 64°C), and extension (3 min at 72°C), and a final elongation at 72°C for 5 min. The 1.2 kb PCR product was electrophoresis in a 0.8% agarose gel in TBE buffer at 60 volts. The PCR product was recovered from the gel by using QIAquick PCR Purification Kit. The purified PCR products were checked by agarose gel electrophoresis before used. The purified double stranded 1.2 kb PCR products were ligated into pGEM-T Easy Vector System and transformed into *E. coli* DH5α by gene pulse II at the same conditions as described above. The 1.2 kb PCR products were subcloned into pUC118 before sequencing. The nucleotide sequencing and analysis were done as mention above. RT-PCR was performed with total RNA of wild type and NTG mutant strains as a template by using the same primers as normal PCR. RT-PCR condition was also done as described above with 20, 30, and 40 cycles, respectively. The PCR products were analyzed by electrophoresis in a 0.8% agarose gel.

5.4 Polyacrylamide gel electrophoresis and ADH activity staining. Sodium dodecyl sulfate-polyacrylamide gel electrophoresis (SDS-PAGE) was performed with a 12.5% acrylamide by the method of Laemmli *et al.*, 1970. Before application, protein samples were mixed with 10 µl of sample buffer and heated at 60°C for 30 min. Then, the treated samples were put on a SDS-PAGE slab gel. The electrophoresis was carried out at 5 and 10 mA for stacking and separating gels, respectively. The standard pre-stained protein marker (BioRad) used for estimation of molecular weight contains phosphorylase *B* (110,000 daltons), bovine serum albumin (77,000 daltons), ovalbumin (50,500 daltons), carbonic anhydrase (35,200 daltons), soybean trypsin inhibitor (28,100 daltons), and lysozyme (21,200 daltons). After electrophoresis, protein staining of the gel was done with Coomassie brilliant blue R-250 for 30 min and then destained with destaining buffer overnight.

Disc gel electrophoresis was performed under the same conditions as described by Davis, 1964, using a 5% polyacrylamide for stacking gel, 7.5% polyacrylamide for separating gel and Tris-glycine buffer (pH 8.3). Protein samples were mixed with sample buffer before application. Two NAD-dependent ADHs activities were detected by dipping the gel in a 100 mM glycine-NaOH (pH 8.5), 0.1 mM NAD, 0.1 M ethanol, nitroblue tetrazolium (NBT), and

phenazine methosulfate (PMS). After incubation in the dark condition, the reaction was stopped by transferring the gel into 7% acetic acid solution.

5.5 Heme staining. The protein samples containing 50 µg of protein were mixed with sample buffer for heme staining and then heated at 60°C for 30 min. The treated samples were put on a 12.5% SDS-PAGE as described above. After electrophoresis, the gel was stained in the staining buffer consists of 9 mg of TMB2 (3,3', 5, 5'-tetramethylbenzidine) in 6 ml of methanol and 14 ml of 0.25 M acetate buffer (pH 5.0) with gently shake at room temperature for 1-2 h. The blue color was developed by adding 60 µl of hydrogen peroxide into the staining buffer. The reaction was stopped by put the gel in destaining buffer containing 6 ml of isopropanol and 14 ml of 0.25 M acetate buffer (pH 5.0) with gently shake at room temperature overnight.

5.6 Immunoblot analysis. Immunoblotting of ADH was performed as described by Burnette, 1981, with some modifications. The protein samples (50 µg of protein) in the gel after SDS-PAGE were transferred electrophoretically onto polyvinylidene difluoride (PVDF) membrane, which had been immersed in methanol for 20 sec. The transferring was done in Tris-glycine buffer (pH 8.3) at 100 mA for 4 h. The membrane was blocked with 3% gelatin in Tris buffered-saline (TBS; 20 mM Tris-HCl, 500 mM NaCl, pH 7.5) overnight. The membrane was washed with TBS containing 0.05% Tween 20 with shaking at room temperature for 10 min for three times. The membrane was further incubated with 1% gelatin in TBS containing antibody raised against ADH for 2 h. The membrane was washed again and incubated with 1% gelatin in TBS containing protein A-peroxidase conjugate for 2 h. After the membrane was washed with TBS containing 0.05% Tween 20, the enzyme band was visualized by the addition of color reagent and hydrogen peroxide in TBS. The reaction was stopped by washing the membrane with distilled water for several times. The results were photographed to provide a permanent record.

5.7 Enzyme assays. All enzyme assays from the membrane fractions were performed at 25°C as follows. Membrane-bound ADH (EC 1.1.99.8) and ALDH (EC 1.2.99.3) were measured colorimetrically with potassium ferricyanide as an electron acceptor described by Adachi et al., 1978a with a slightly modification (Matsushita et al., 1995). The rate of reduction of ferricyanide to

ferricyanide gives a quantitative amount of ethanol oxidized. One unit of enzyme activity was defined as the amount of enzyme catalyzing the oxidation of 1 μmol of ethanol per min. The ethanol and acetaldehyde oxidase activities were also measured with the membrane by using a Clark type oxygen electrode. One unit of these enzyme activities was defined as the amount of enzyme catalyzing the formation or consumption of 1 μmol of reaction product or substrate per min. NADH-oxidase activity was measured by following the decrease of NADH. The enzyme activity was calculated with a millimolar extinction coefficient of 6.22 at 340 nm and expressed as 1 μmol of NADH oxidized per min.

The soluble fractions were also measured for the several enzyme activities as follows. The following enzyme assays were done at 35°C spectrophotometrically by measuring the formation or disappearance of NAD(P)H. NAD-dependent ADH (EC 1.1.1.1) activity was measured according to the method describe by Bergt and Gutmann, 1974 with slight modification (Chinnawirotpisan et al., 2003a). The formation of NADH follows the oxidation of ethanol to acetaldehyde (forward reaction), while the disappearance of NADH does the reduction of acetaldehyde to ethanol (reverse reaction). Two different NAD-dependent ADHs were determined as follows. For NAD-dependent ADH I, the reaction mixture (1 ml) for the forward reaction contained 100 mM glycine-NaOH (pH 8.5), 100 mM ethanol, and 0.1 mM NAD, while the assay mixture for the reverse reaction (1 ml) contained 100 mM KPB (pH 6.5), 10 mM acetaldehyde, and 0.1 mM NADH. For NAD-dependent ADH II, the forward reaction mixture (1 ml) contained 100 mM glycine-NaOH (pH 8.5), 100 mM ethanol, and 0.1 mM NAD, while that for the reverse reaction (1 ml) contained 100 mM 2-morpholinoethanesulfonic acid (MES) buffer (pH 6.0), 100 mM acetaldehyde, and 0.1 mM NADH. The reaction was started by the addition of enzyme solution. NADP-dependent aldehyde dehydrogenase (EC 1.2.1.4) activity was measured by the method of Adachi et al., 1980. Acetate kinase (EC 2.7.2.1) was measured by the reverse reaction with acetyl phosphate as the primary substrate in the presence of ADP and inorganic phosphate as described by Nishimura and Griffith, 1981, in which ATP generated was measured by coupling reaction with hexokinase and D-glucose-6-phosphate dehydrogenase. Acetyl-CoA synthetase (EC 6.2.1.1) was measured by the reverse reaction with acetyl-CoA as the primary substrate in the presence of AMP and pyrophosphate, in which the same coupling reaction as above was used to measured ATP generated by the method of Frenkle and Kitchens, 1961. NAD-dependent isocitrate dehydrogenase (EC 1.1.1.42) (α-ketoglutarate

formation) was measured by a modification of the method of Williamson and Corkey, 1969. The reaction was started by adding DL-isocitrate, which had been neutralized previously. These enzyme activities were calculated with a millimolar extinction coefficient of 6.22 at 340 nm and expressed as 1 µmol of NAD(P)H oxidized or NAD(P) reduced per min. Isocitrate lyase (EC 4.1.3.1) was measured by the method of Yoshida et al., 1995. One unit of enzyme activity was defined as the amount of enzyme catalyzing the formation or consumption of 1 µmol of reaction product or substrate per minute.

RESULTS AND DISCUSSION

1. Molecular taxonomy by using 16S ribosomal DNA sequencing

The chromosomal DNA from *Acinetobacter* sp. was used as the template for 16S rDNA amplification by PCR with the forward and reverse primers as described in Materials and Methods. The PCR amplified 16S rDNA was analyzed in 0.8% agarose gel electrophoresis. The amplified 16S rDNA fragment was ~1.5 kb PCR product, which its size corresponded well with the size of 16S rDNA (Figure 1A). The amplified 16S rDNA fragment was recovered from the gel and then ligated with pGEM-T Easy vector. The ligation product was introduced into *E. coli* DH5α by electroporation. The obtained recombinant plasmid was digested with *Eco*RI and subcloned into pUC118. The selected recombinant plasmids were determined for their nucleotide sequences as shown in Figure 1B. The summary of the percentage of 16S rDNA sequence similarity of SKU1108 and type strains were shown in Table 1. The alignment of 16S rDNA sequences of SKU1108 to 16S rDNA genes of *A. pasteurianus* showed the highest similarity percentage of 99.06. Based on 16S rDNA sequences alignment, the unrooted phylogenetic tree (Figure 2) was constructed from evolutionary by using the neighbor-joining method.

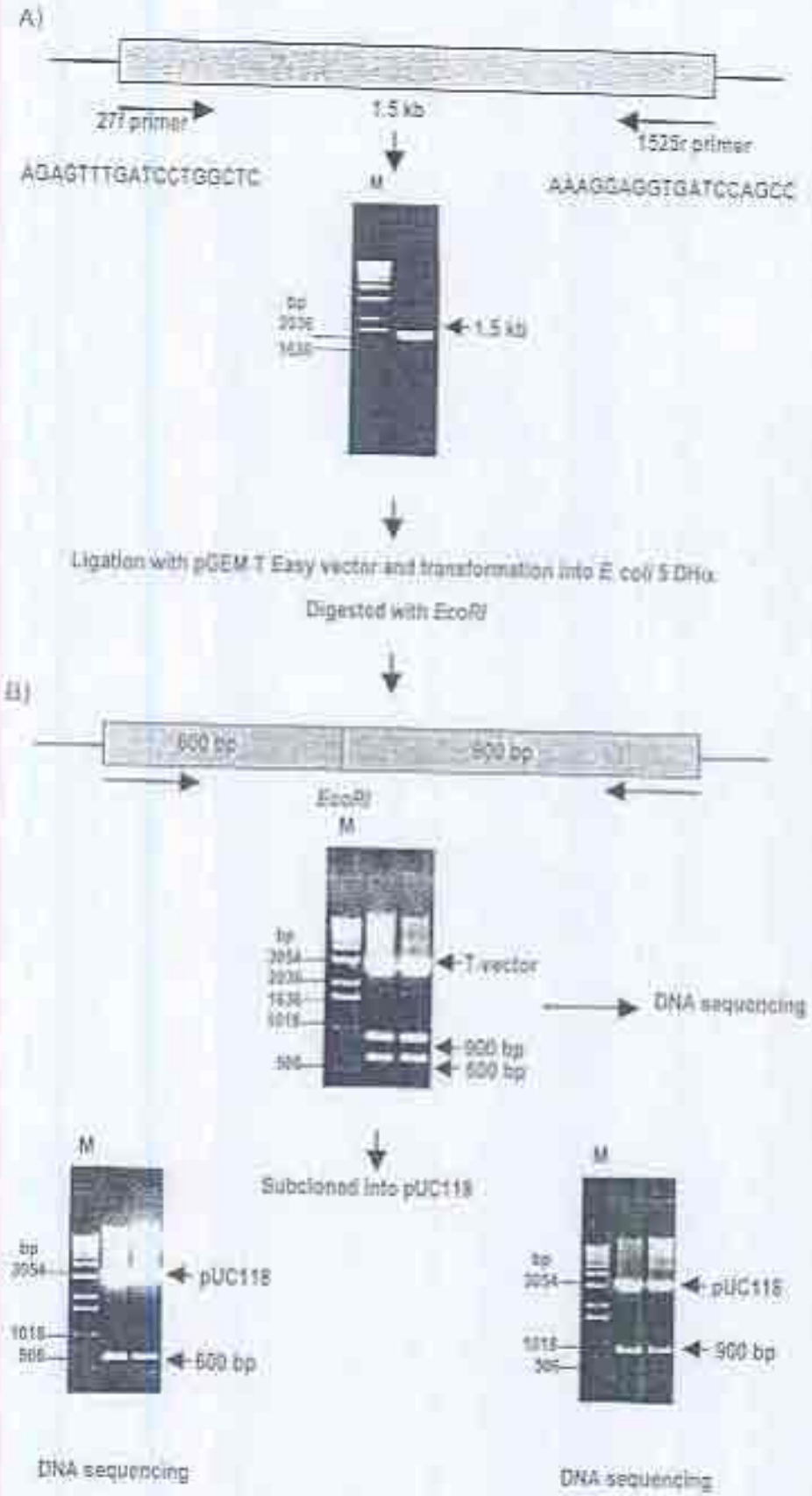

Figure 1 Agarose gel electrophoresis of 1.5 kb PCR amplified 16S rDNA (A) and schematic diagram for 16S rDNA sequencing (B).

Table 1 16S rDNA sequence similarity of acetic acid bacteria to type strains of *Acetobacter*

Strain	% 16S rDNA sequence similarity SKU1108
Acetobacter pasteurianus (X71863)	99.59
Acetobacter aceti (X74066)	98.96
Acetobacter liquefaciens (X75617T)	95.81
Acetobacter diazotrophicus (X75618)	95.14
Acetobacter methanolicus (D32770)	95.00
Acetobacter xylinum (X75619)	94.87
Acetobacter hansenii (X75620)	94.46

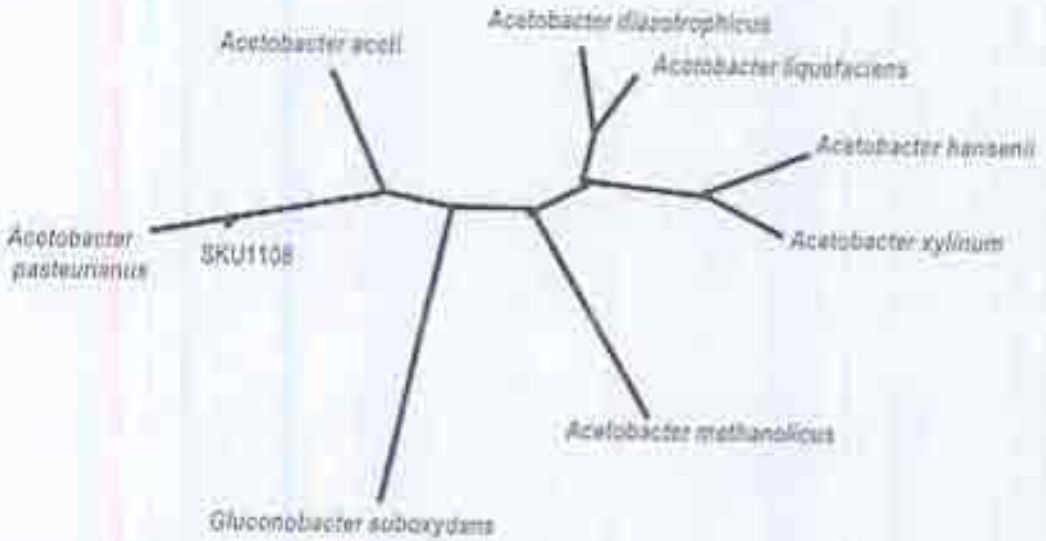

Figure 2 16S rDNA-based tree reflecting the phylogenetic position of *Acetobacter* sp. SKU1108 strain and the related acetic acid bacteria. The analysis was done by using the following sequence from GenBank: *Acetobacter pasteurianus*, *Acetobacter aceti*, *Acetobacter liquefaciens*, *Acetobacter diazotrophicus*, *Acetobacter methanolicus*, *Acetobacter xylinum*, *Acetobacter hansenii* and *Gluconobacter oxydans*.

2. Purification and characterization of membrane-bound quinoprotein alcohol dehydrogenase (PQQ-ADH)

2.1 Characterization of crude PQQ-ADH

A. pasteurianus SKU1108 has been shown to have an ability to produce high amount of acetic acid and also to possess high tolerance to acetic acid even at higher temperature (Saeki *et al.*, 1997a). Such ethanol oxidation and acetic acid resistance have been suggested to be closely related each other, and to be related to quinoprotein ADH. In this study, it was found that PQQ-ADH in membrane fraction of *A. pasteurianus* SKU1108 exhibited higher tolerance to acetic acid than *A. lovaniensis* IFO3284 as shown in Figure 3A. In addition, effect of sodium acetate concentration and pH against PQQ-ADH activity were also investigated with both membrane fractions (Figure 3B and C). In contrast, it seemed to be that PQQ-ADH in membrane fraction of *A. lovaniensis* IFO3284 possessed higher tolerance to sodium acetate than *A. pasteurianus* SKU1108. The possible reason for explaining this phenomenon is that high concentration of sodium acetate leads to an increase in pH. Based on the effect of pH, remaining activity of PQQ-ADH in membrane fraction of *A. lovaniensis* IFO3284 increased at higher pH. So, PQQ-ADH in membrane fraction of *A. lovaniensis* IFO3284 is stable at pH >4.5, whereas PQQ-ADH in membrane fraction of *A. pasteurianus* SKU1108 is stable at pH <4.5. Therefore, in order to elucidate that the acetic acid tolerance depend on the PQQ-ADH itself or other membrane components, PQQ-ADH was purified from *A. pasteurianus* SKU1108 to compare with the purified PQQ-ADH from *A. lovaniensis* IFO3284.

A)

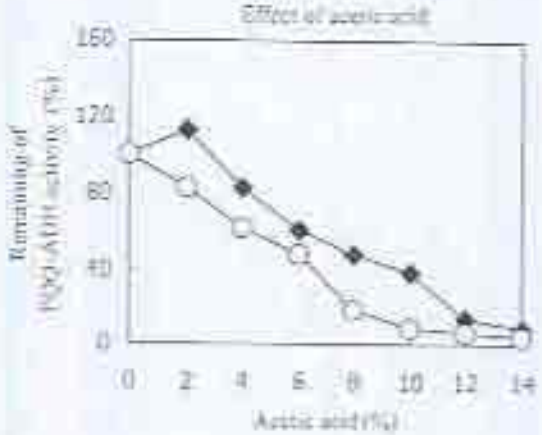

B)

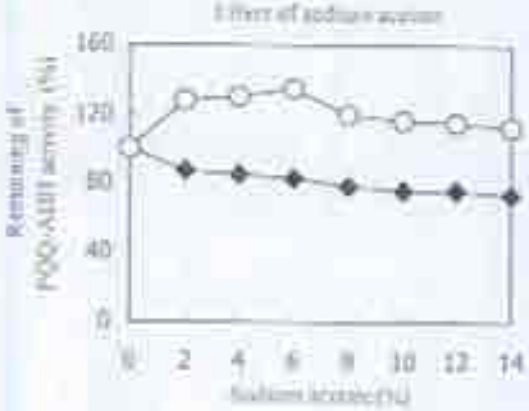

C)

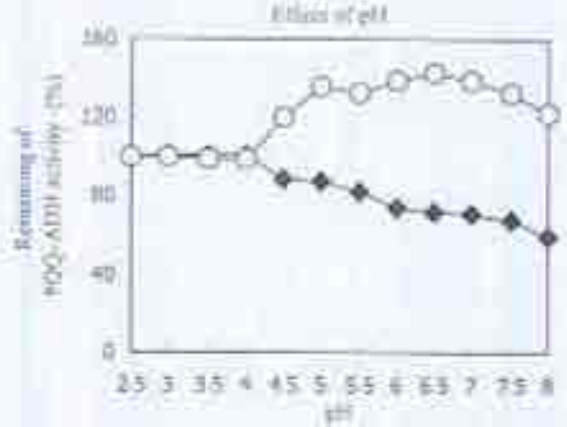

Figure 3. Effect of acetic acid, sodium acetate, and pH against PQQ-ADH activity on the membrane fraction of *A. pasteurianus* SKU1108 (○-) and *A. lovaniensis* IFO 3284 (◆-).

2.2 Purification of PQQ-ADH

All of the PQQ-ADH activity was found in the precipitate after ultracentrifugation of the crude extract from *A. pasteurianus* SKU1108 cultured in the medium containing ethanol. During the purification, enzyme activity against ethanol was measured by ferricyanide dupenol method. The membrane fraction was solubilized with 1% Triton X-100 and a rose-red colored enzyme solution were obtained. The PQQ-ADH activity was purified by two steps columns, which are DEAE-Toyopearl and hydroxyl apatite column chromatographies. DEAE-Toyopearl column is very useful for this purification because almost all protein impurity could be removed from PQQ-ADH as shown in Figure 4. The combined active fractions (no. 87-101) from DEAE-Toyopearl column containing 7.60 mg protein was applied onto a hydroxyl apatite. The elution pattern of hydroxyl apatite column chromatography was shown in Figure 5. The whole enzymic activity was eluted with 150 mM KPB (pH 6.0). The purification of PQQ-ADH is summarized in Table 2. The PQQ-ADH was concentrated around 35-fold with 41% yield.

The purified enzyme fractions of PQQ-ADH obtained from the final step, had a three protein bands in SDS-PAGE (Figure 6A). The relative molecular mass of PQQ-ADH was estimated by SDS-PAGE to be 76 kDa (subunit I), 46 kDa (subunit II) and 18 kDa (subunit III), respectively. It was suggested that the native PQQ-ADH consists of three different subunits, which is similar to almost all of the known PQQ-ADH from other species of acetic acid bacteria. As described above, PQQ-ADH contains four heme *c* moieties per molecule (one in subunit I and the other three in subunit II), thus heme staining was determined with various samples of the purified enzyme (Figure 6B). It was clearly shown that there are two positive bands of heme staining corresponding to subunit I and subunit II.

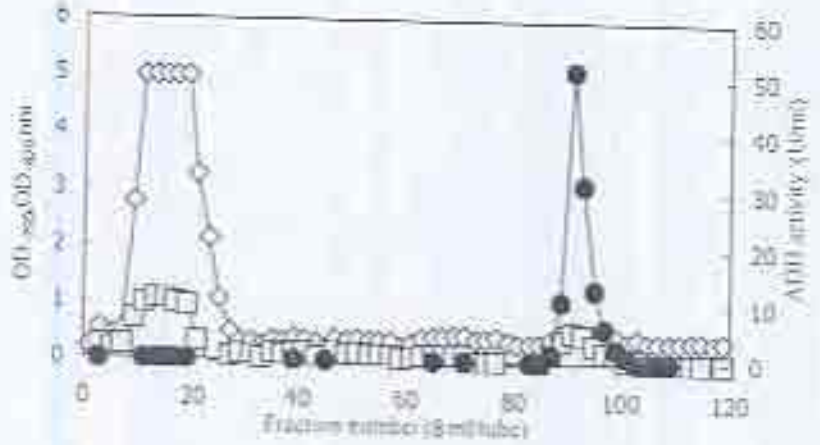

Figure 4 Elution pattern of the DEAE-Toyopearl column chromatography. Enzyme solution containing 110 mg of protein was applied to a DEAE-Toyopearl column equilibrated with 5 mM KPB (pH 6.0) containing 0.1% Triton X-100. The enzyme was eluted with a concave gradient consists of 4 bed volume of 5 mM KPB (pH 6.0) containing 0.1% Triton X-100 and 2 bed volume of 50 mM KPB (pH 6.0) containing 0.1% Triton X-100. Each fraction (8 ml) was analyzed for protein (OD_{280nm}, -◇-), heme (OD_{402nm}, -□-) and (ADH activity, -●-).

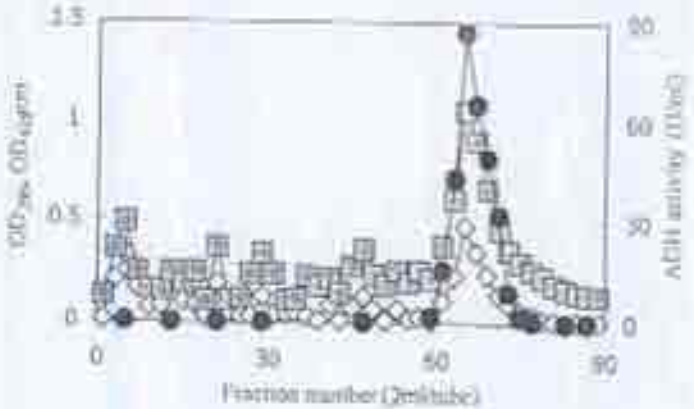

Figure 5 Elution pattern of the hydroxyl apatite column chromatography. The combined active fractions (no. 87-101) from DEAE-Toyopearl column chromatography (7.60 mg of protein was applied to a hydroxyl apatite column equilibrated with 50 mM KPB (pH 6.0) containing 0.1% Triton X-100. The enzyme was eluted with step wise consists of 5 bed volume of 100 mM KPB (pH 6.0) containing 0.1% Triton X-100 and 5 bed volume of 150 mM KPB (pH 6.0) containing 0.1% Triton X-100. Each fraction (2 ml) was analyzed for protein (OD_{280nm}, -◇-), heme (OD_{402nm}, -□-) and (ADH activity, -●-).

Table 2 Purification summary of membrane-bound quinoprotein ADH from *A. pasteurianus* SKU1108

Step	Total activity* (U)	Total protein (mg)	Specific activity (U/mg)	Purification (fold)	Yield (%)
Membrane	1,690	310	5.45	1	100
Solubilized	1,238	110	11.2	2.06	73.2
DEAE-Toyopearl	550	7.60	73.7	13.5	32.5
Hydroxyl apatite	689	3.60	192	35.1	40.8

Note: * Activity was measured by ferricyanide (Duperol methods)

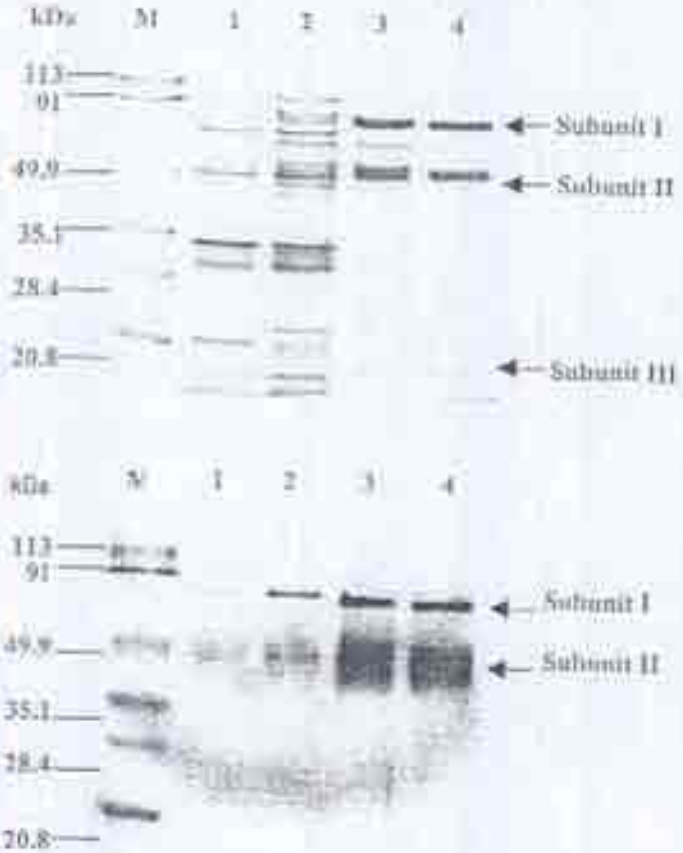

Figure 6 SDS-PAGE of the purified PQQ-ADH from membrane fraction of *A. pasteurianus* SKU1108. PQQ-ADH was treated with SDS sample buffer with (for protein staining) or without (for heme staining) DTT for 30 min at 60°C and applied to a SDS gel containing 12.5% acrylamide. The gels were stained by protein staining (A) and heme staining (B). Lane1: membrane fraction; Lane 2: solubilized membrane fraction; Lane 3: DEAE-Toyopearl active fractions and Lane 4: hydroxyl apatite active fractions. Each lane contained 10 µg of protein.

2.3 Effect of acetic acid, sodium acetate, and pH against PQQ-ADH activity

The nearly purified PQQ-ADH obtained from *A. pasteurianus* SKU1108 and *A. tovanensis* IFO3284 were used to determined the effect of acetic acid, sodium acetate and pH against PQQ-ADH activity. The enzyme solution was incubated in 10 mM KPB (pH 6.0) containing various concentration of acetic acid for 5 min on ice and then the sample was taken for PQQ-ADH activity assay by ferricyanide dyteral method. The effect of sodium acetate and pH were also determined by using the same procedure. As the results (Figure 7), there is no different of ADH activity between the purified PQQ-ADH from SKU1108 and IFO3284 in acetic acid, sodium acetate, and pH, respectively. Therefore, it was suggested that the membrane fraction of SKU1108 have some components, which have acetic acid resistance property. In order to clarify that PQQ-ADH itself or other component in the membrane possesses acetic acid resistance ability, the detergent (Triton X-100) should be removed from the purified enzyme or purification of other membrane components such as phospholipid followed by reconstitution of those components. The alternative method is to construct acetic acid sensitive mutant or PQQ-ADH deficient mutant.

A)

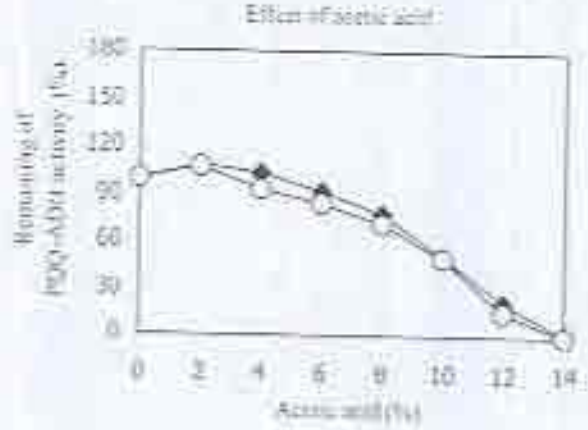

B)

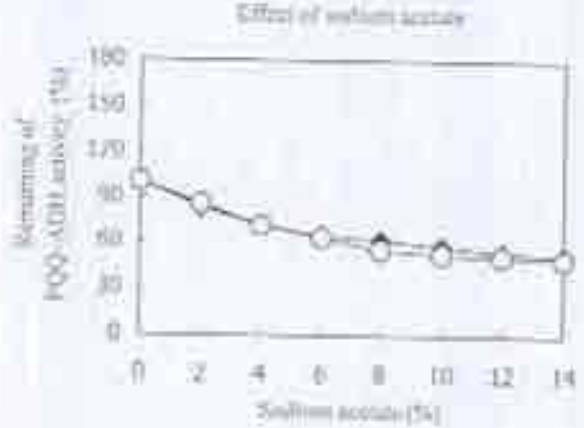

C)

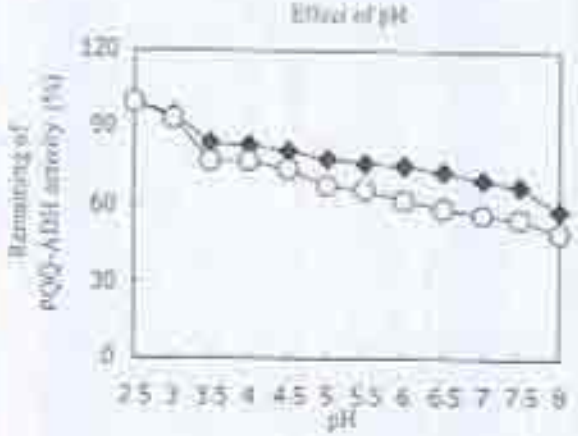

Figure 7 Effect of acetic acid, sodium acetate, and pH against PQQ-ADH activity in the purified PQQ-ADH from *A. pasteurianus* SKU1108 (○) and *A. lovaniensis* IFO3284 (◆).

3. Characterization of NTG mutant

In order to clarify the function of PQQ-ADH, PQQ-ADH deficient mutants were isolated from *A. pasteurianus* SKU1108 by NTG treatment. After NTG mutagenesis, colonies deficient in ethanol-oxidizing ability were screened by the absence of clear zone on ethanol-$CaCO_3$ plate. The selected 8 mutants were characterized and classified into two groups. The first group consisting of CN6-1 and CN6-2 exhibited complete loss in ethanol-oxidizing ability and acetic acid resistance. The second group consists of CN6-3 to CN6-8, which exhibited low ethanol-oxidizing ability. Finally, PQQ-ADH deficient mutant, CN6-2 was selected for further analysis (Jotiwattana, 2001).

3.1 Comparison of *adh* mRNA synthesis by RT-PCR

RT-PCR analysis of RNA prepared from *A. pasteurianus* SKU1108 and CN6-2 were carried out to investigate whether mRNA of adh gene was synthesized in CN6-2 or not. Two specific primers, primer C and D for amplification of 1.2 kb truncated *adhA* gene were designed and used in PCR and RT-PCR. As shown in Figure 8, the 1.2 kb RT-PCR product was clearly detected from 30 and 40 cycles of PCR of both SKU1108 and CN6-2 (lane 2-3 and 5-6). This result implicated that the mutation site did not affect the transcription of *adh* gene because *adh* mRNA could be detected in CN6-2 by RT-PCR. The DNase treated RNA from SKU1108 and CN6-2 in lane 7 and 8 were carried out to confirm that no contaminated DNA existed in RNA sample used in RT-PCR. Thus the RT-PCR amplified products were really obtained from mRNA not contaminated DNA.

3.2 Nucleotide sequences of PCR-amplified adhA gene

The nucleotide sequence of PCR-amplified 1.2 kb *adhA* gene was determined (Figure 9). The obtained nucleotide sequence was analyzed and compared with SKU1108 strain, it was found that there is a single deletion of one base (G) at the position 1674 in *adhA* gene of CN6-2, causing frame shift and producing nonsense mutation by TAG codon at the position 1906, which creates 10 different amino acid sequences at the position from 582 to 591 and stop at the position 592 (Figure 10). The result of this mutation leads the deletion of 150 amino acid residues or 16 kDa protein in PQQ-ADH subunit I.

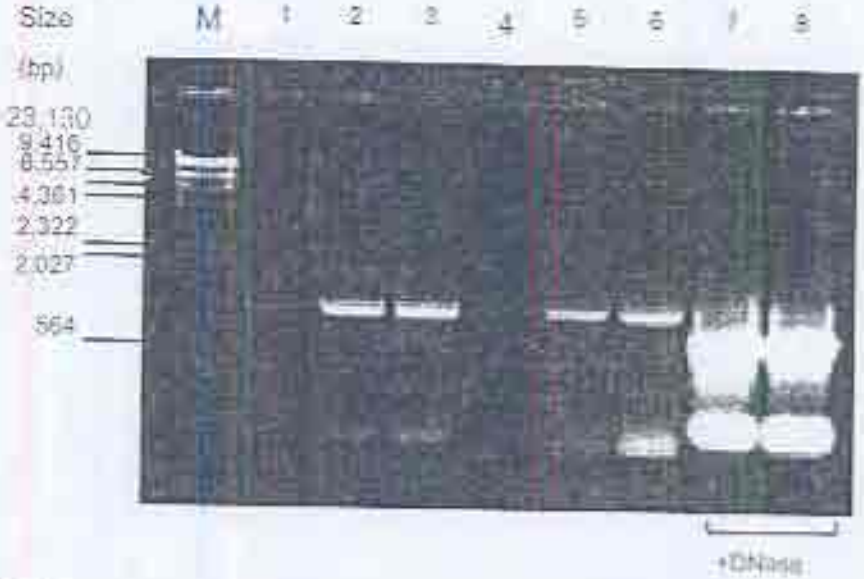

Figure 8 Agarose gel electrophoresis of RT-PCR of mRNA isolated from *A. pasteurianus* SKU1108 and CN6-2 by using primer C and D. Lane M: λ DNA/*Hin*dIII fragments; Lane 1-3: 1.2 kb RT-PCR amplified product of *A. pasteurianus* SKU1108 from 20, 30 and 40 cycles, respectively; Lane 4-6: 1.2 kb RT-PCR amplified product of CN6-2 from 20, 30 and 40 cycles, respectively and Lane 7-8: total RNA of *A. pasteurianus* SKU1108 and CN6-2 treated with DNase, respectively.

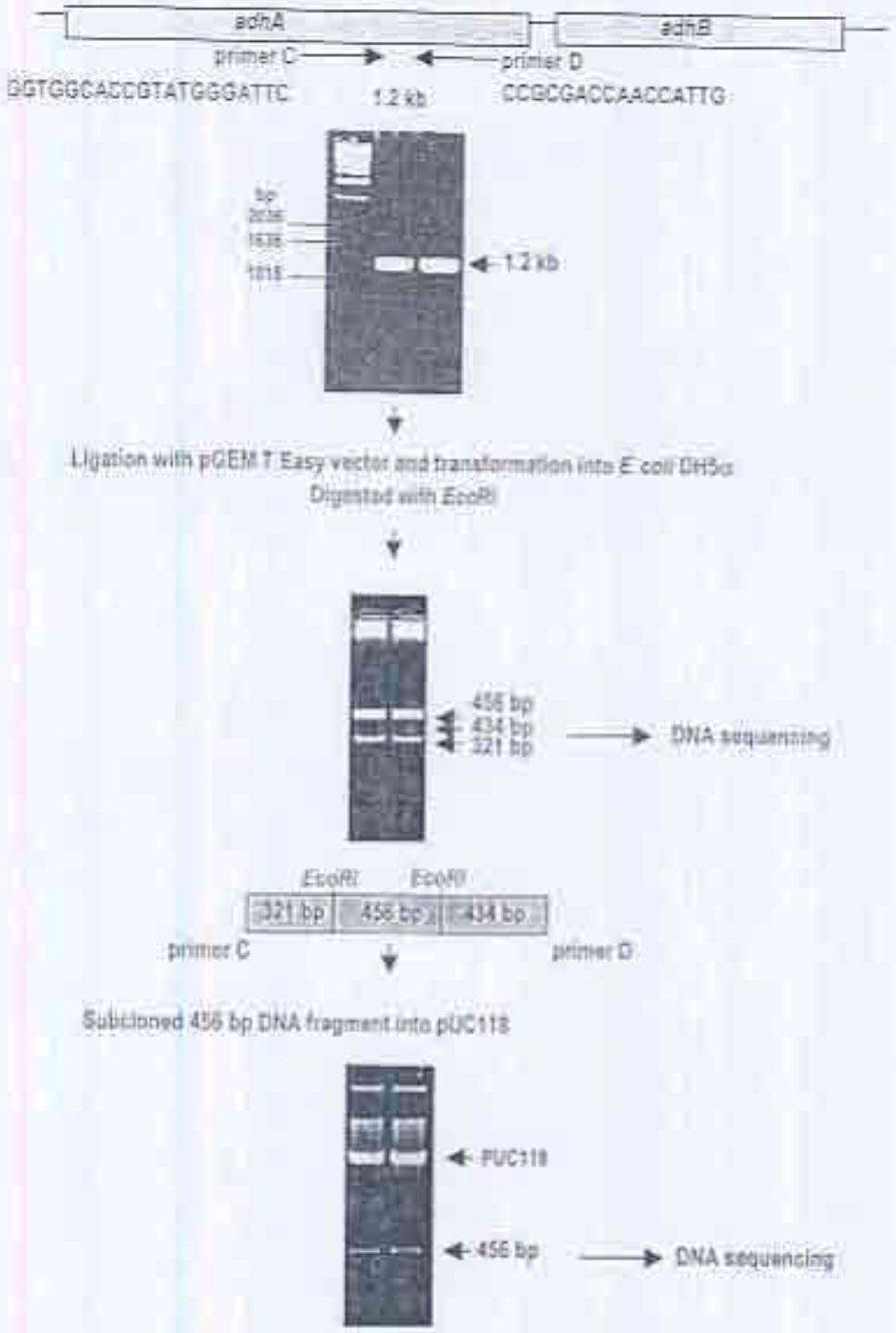

Figure 3 Schematic diagram for sequencing of 1.2 kb *adhA* gene of *A. pasteurianus* SKU1108 and CN6-2 NTG mutant strain

A)

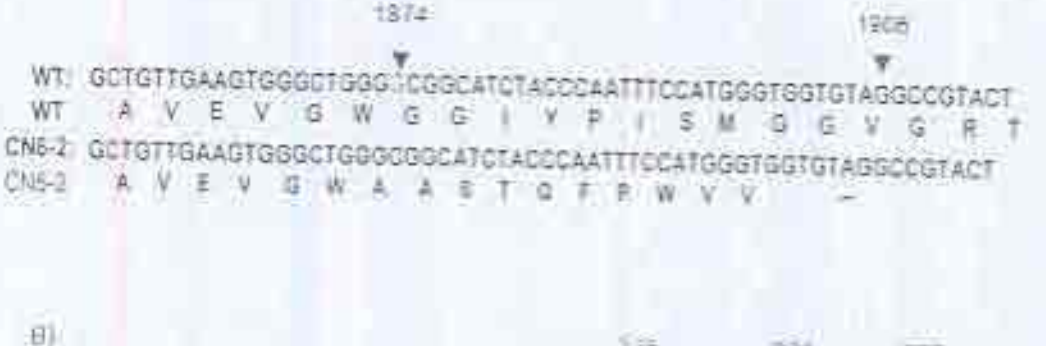

B)

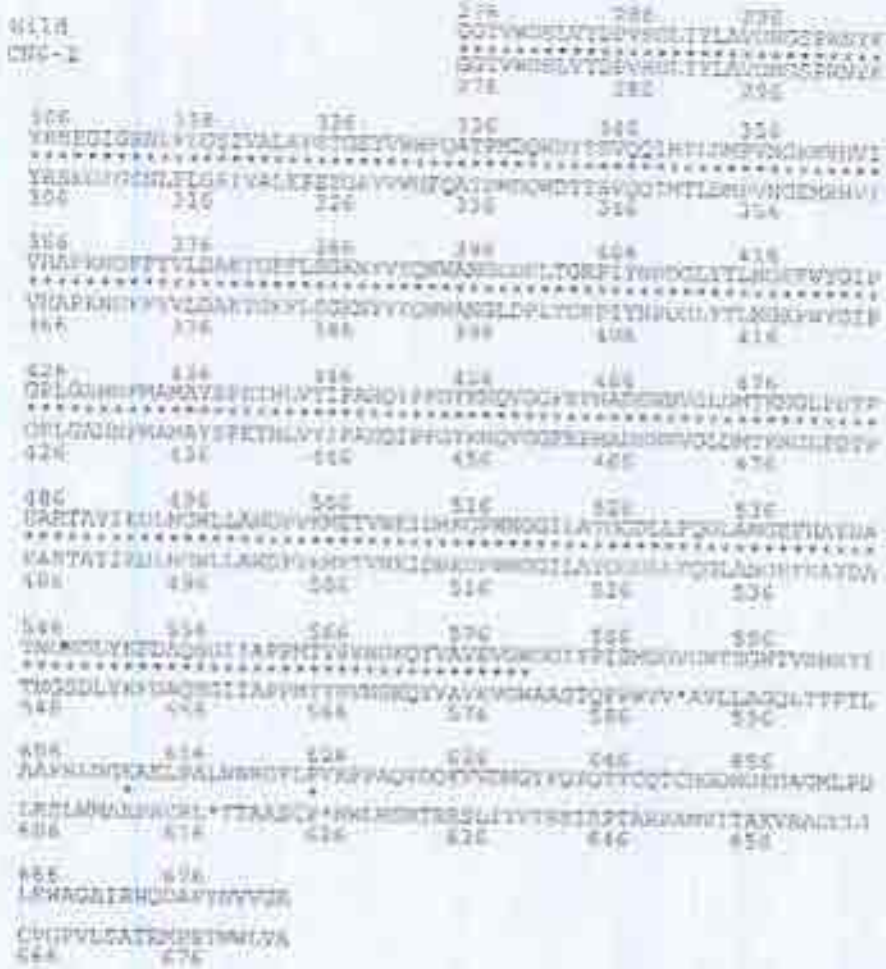

Figure 10 Amino acid sequence deduced from 1.2 kb *adhA* gene of *A. plasteuriarius* CN6-2 NTG mutant strain. One base (G) deletion at position 1574 indicated by (▼ was observed in 1.2 kb *adhA* gene of CN6-2 NTG mutant strain (A) and (B) amino acid sequence of 1.2 kb *adhA* gene of CN6-2 NTG mutant strain.

3.3 Comparison of PQQ-ADH activity and immunoblot analysis of PQQ-ADH subunit

The ethanol-oxidizing ability of *A. pasteurianus* SKU1108 and CN6-2 NTG mutant strain were compared on YPGD medium supplemented with 2% ethanol and 0.5% $CaCO_3$ (Figure 11). PQQ-ADH deficient mutant CN6-2 could not produce any clear zone when compared with the wild strain.

Figure 11 Comparison of clear zone formation of *A. pasteurianus* SKU1108 and CN6-2 NTG mutant strain. Two strains were spotted on YPGD medium containing 0.5% $CaCO_3$ and 2% ethanol and incubated for 24 h at 30°C.

The enzyme activities involved in ethanol oxidation were assayed in both membrane and soluble fractions as shown in Table 3. In the wild-type strain, both membrane-bound ADH and ALDH activities were induced by the addition of ethanol into the culture medium, while the NAD-dependent ADH (NAD-ADH) was very low. In contrast, both membrane-bound ADH and ALDH activities were showed very low activities when compared with the wild strain, whereas the NAD-ADH activity was induced in the ethanol containing medium. It may be supported by the above figure exhibited that CN6-2 NTG mutant strain could not produce clear zone in ethanol $CaCO_3$ plate. Therefore, this strain did have any membrane-bound ADH and ALDH activities.

Table 3 Summarization of enzyme activities (U/mg of protein) involved in ethanol oxidation

Stain/ethanol (%)	NAD-ADH (forward)	NAD-ADH (reverse)	Membrane-bound ADH	Membrane-bound ALDH
SKU1108 (0% ethanol)	0.016	0.731	2.43	5.20
SKU1108 (4% ethanol)	0.016	0.659	6.26	7.08
CN6-2 (0% ethanol)	0.096	1.42	0.018	0.021
CN6-2 (4% ethanol)	0.324	14.6	0.031	0.053

Membrane and soluble fractions were prepared from two different growth conditions of wild strain SKU1108 and NTG mutant CN6-2 grown in YPGD medium supplemented with 4% ethanol. NAD-ADH, NAD-dependent alcohol dehydrogenase; the formation of NADH follows the oxidation of ethanol to acetaldehyde (forward reaction), while the disappearance of NADH does the reduction of acetaldehyde to ethanol (reverse reaction) by using soluble fraction. Membrane-bound ADH and ALDH activities were assayed by ferricyanide dupanol methods. The enzyme activity is given as the specific activity (U/mg of protein).

The localization of PQQ-ADH in CN6-2 NTG mutant strain was also determined by using immunoblot analysis with both membrane and soluble fractions of SKU1108 and CN6-2. The positive bands of PQQ-ADH subunits were performed by using antisera of PQQ-ADH have been purified from *A. aceti*. All three subunits of PQQ-ADH were found in the membrane fraction of wild strain, while no significantly appreciable bands for subunit I, II and III were detected in the membrane faction of CN6-2 strain. In contrast, in the soluble fraction, a relative high amount of a truncated subunit I was seen together with subunit III in CN6-2 strain (Figure 12). The truncated subunit I of CN6-2 strain was expected to be due to frame-shift mutation as described previously.

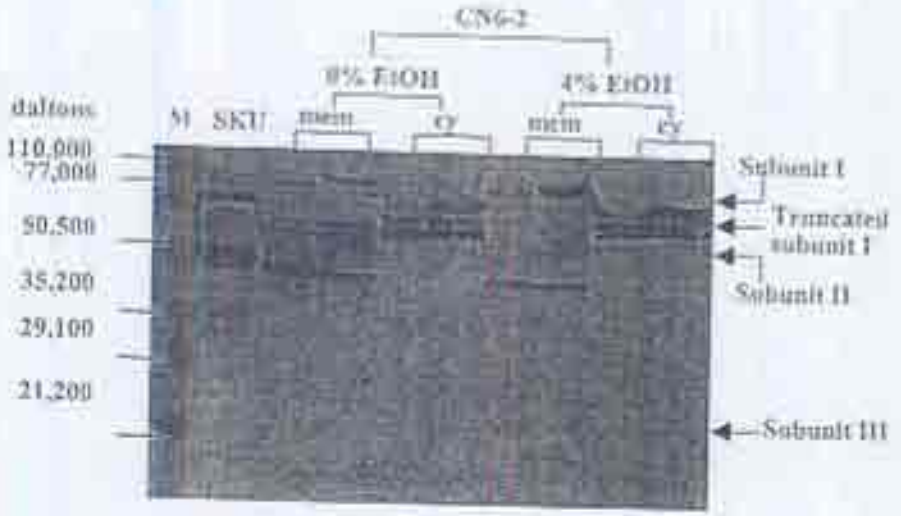

Figure 12 Immunoblot analysis of PQQ-ADH. Immunoblot of membrane and soluble fractions of *A. pasteurianus* SKU1108 and CN6-2 NTG mutant grown in YPGD medium supplemented with 4% ethanol for 48 h. SDS-PAGE and blotting were done as described in Materials and Methods with 50 □g of protein (SKU1108 25 □g of protein). Antisera used are anti-PQQ ADH from *A. aceti*.

3.4 Comparison of growth and acetic acid production

The growth and acetic acid production were compared with *A. pasteurianus* SKU1108 and CN6-2 NTG mutant strain in YPGD medium supplemented with 4% ethanol at 30°C for 10 days (Figure 13). *A. pasteurianus* SKU1108 rapidly oxidized ethanol without a lag time and accumulated acetic acid in the culture medium. The accumulated acetic acid was further consumed after several days. In contrast, in the CN6-2 NTG mutant strain, could not produce any acetic acid in the culture medium even long incubation time. Interestingly, in CN6-2 NTG mutant strain, the addition of ethanol in the culture medium significantly enhanced the growth, concomitant with the increased of NAD ADH in the cytoplasm but no acetic acid production, leading the question why and how CN6-2 strain utilized ethanol in the culture medium despite of no ethanol-oxidizing ability. Therefore, the NAD ADH activity that increased dramatically in the NTG mutant cultured in ethanol-containing medium was used for further purification.

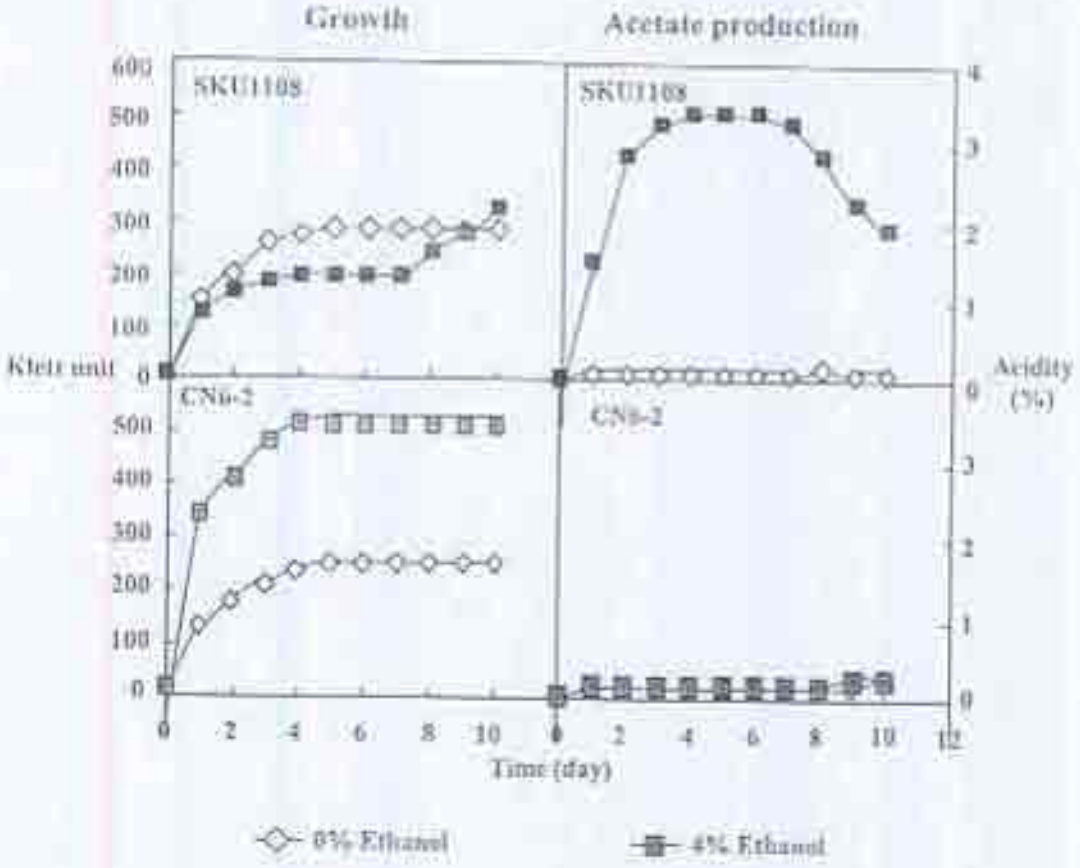

Figure 13 Time course of the growth and acetic acid production. *A. pasteurianus* SKU1108 and CN6-2 NTG mutant were cultured in YPGD medium supplemented with 4% ethanol.

4. Purification and characterization of two NAD-dependent alcohol dehydrogenases (NAD-ADHs) induced in PQQ-ADH deficient mutant

4.1 Purification of two NAD-dependent ADHs

All of NAD-dependent ADH activity was found in the supernatant after ultracentrifugation of the crude extract from *A. pasteurianus* CNR-2 NTG mutant strain. This soluble fraction was directly applied onto a DEAE-Toyopearl column I (about 1 ml of bed volume per 3 mg of protein), equilibrated with 50 mM KPB (pH 7.5). Under these conditions, most of the enzyme activity was not absorbed onto the column (Figure 14). During the purification, enzyme activity against acetaldehyde was measured (reverse reaction of NAD-dependent ADH). The combined pass through fractions (no. 13-31) having the enzyme activity was dialyzed and loaded onto an alternative column of DEAE-Toyopearl equilibrated with 5 mM KPB (pH 7.5). The column was washed and then eluted by a linear gradient of 5 to 50 mM KPB (pH 7.5). As shown in Figure 15, the elution pattern of the crude enzyme from a DEAE Toyopearl column II showed that there were two obvious protein peaks, which contained NAD-dependent ADH activity. The peak constituted from fraction (no. 129-157) was eluted at 35 mM KPB (pH 7.5) and showed an activity preference for primary alcohol designated as ADH I. The combined active fractions from this peak was dialyzed and applied onto a hydroxyl apatite column. The elution pattern of this column was shown in Figure 16. The combined active fraction (no. 125-175) was concentrated by ultrafiltration, dialyzed and loaded onto a DEAE-Toyopearl column III. The elution pattern of this column was shown in Figure 17.

The second protein peak contained the activity was designated as ADH II, pass through a DEAE-Toyopearl column II. The combined active fraction (no. 11-43) was directly applied onto a hydroxyl apatite column and almost all of the enzyme activity was eluted with 100 mM KPB (pH 7.5) as shown in Figure 18. The combined active fraction (no. 105-125) was concentrated and dialyzed with 50 mM KPB (pH 7.5). The dialysate was applied onto a Superdex S-200 equilibrated with the same buffer. The elution pattern from this column was shown in Figure 19. ADH II activity was easily lost during the column chromatographies, which could be stabilized by the addition of DTT and $MgCl_2$ in the column buffer. The purification of two NAD-dependent ADHs are summarized in Table 4. ADH I was enriched around 35-fold with a 15% yield, while ADH II was enriched around 21-fold with 7% yield.

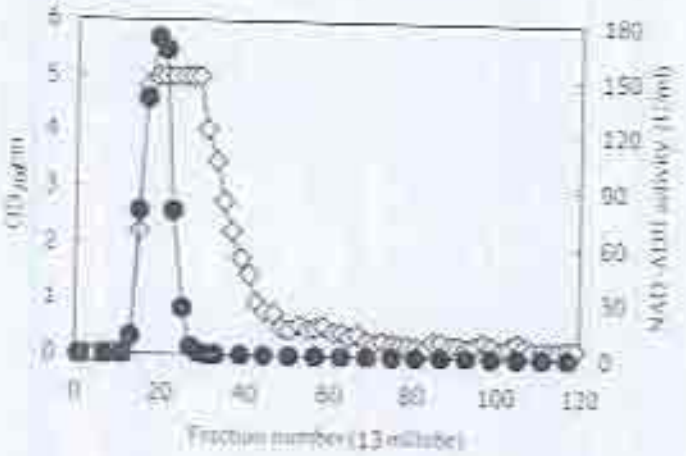

Figure 14 Elution pattern of NAD-dependent ADH I on DEAE-Toyopearl I column chromatography. The resulting supernatant after ultracentrifugation contained 1,830 mg of protein was put directly on a DEAE-Toyopearl I column equilibrated with 50 mM KPB (pH 7.5). Most of the enzyme activity was not absorbed onto the column. Each fraction (13 ml) was analyzed for protein (OD_{280}nm, —◇—) and NAD-ADH I activity (—●—).

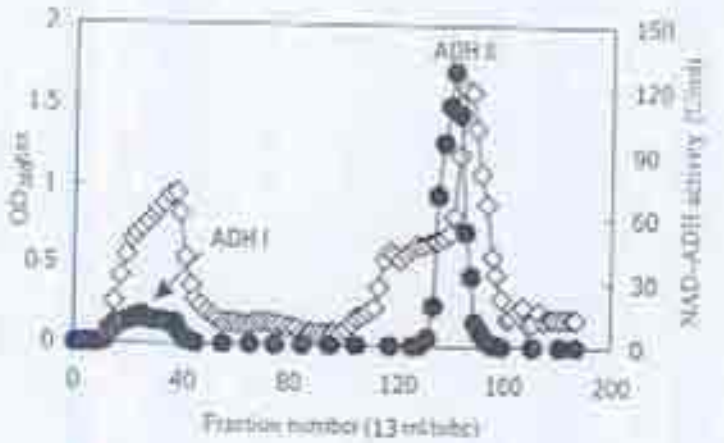

Figure 15 Elution pattern of two NAD-dependent ADH I and ADH II on DEAE-Toyopearl column chromatography II. The combined active fraction from DEAE-Toyopearl column I (no. 42-74) contained 829 mg of protein was applied on a DEAE-Toyopearl column II equilibrated with 5 mM KPB (pH 7.5). The protein was eluted by linear gradient from 5 to 50 mM KPB (pH 7.5). Each fraction (13 ml) was analyzed for protein (OD_{280}nm —◇—) and NAD-ADH activity (—●—).

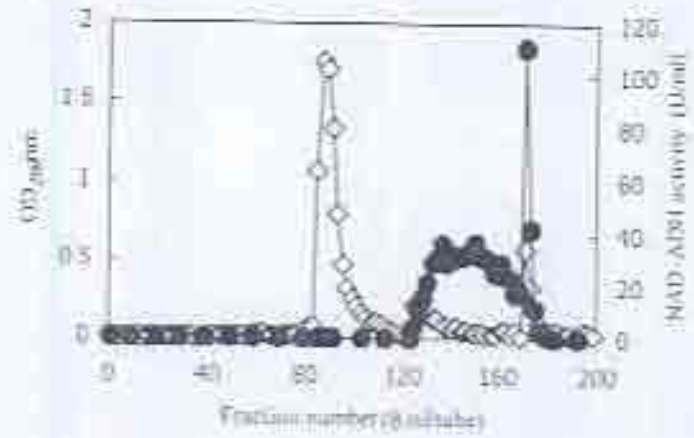

Figure 16 Elution pattern of NAD-dependent ADH I on hydroxyl apatite column chromatography. The combined active fraction from DEAE-Toyopearl column II (no. 129-157) contained 282 mg of protein was applied on a hydroxyl apatite column equilibrated with 50 mM KPB (pH 7.5). The protein was eluted stop wise consists of 50, 100 and 500 mM KPB (pH 7.5). Each fraction (6 ml) was analyzed for protein (OD_{280}nm, —◇—) and NAD-ADH activity (—●—).

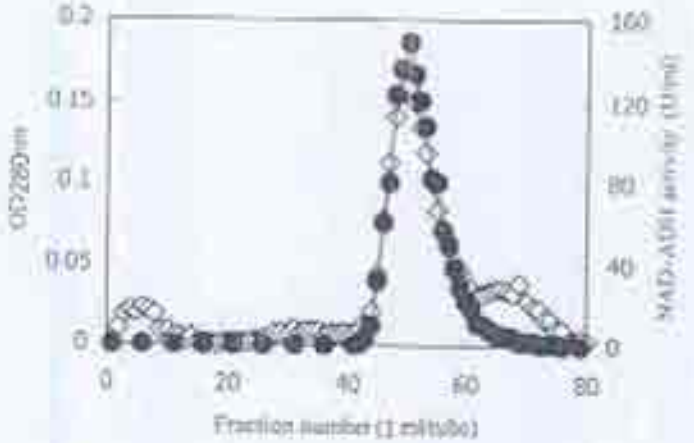

Figure 17 Elution pattern of NAD-dependent ADH I on DEAE-Toyopearl column chromatography III. The combined active fraction from hydroxyl apatite column (no. 125-175) contained 24.2 mg of protein was applied on a DEAE-Toyopearl column equilibrated with 10 mM KPB (pH 7.5). The protein was eluted by linear gradient from 10 to 40 mM KPB (pH 7.5). Each fraction (1 ml) was analyzed for protein (OD_{280}nm, —◇—) and NAD-ADH activity (—●—).

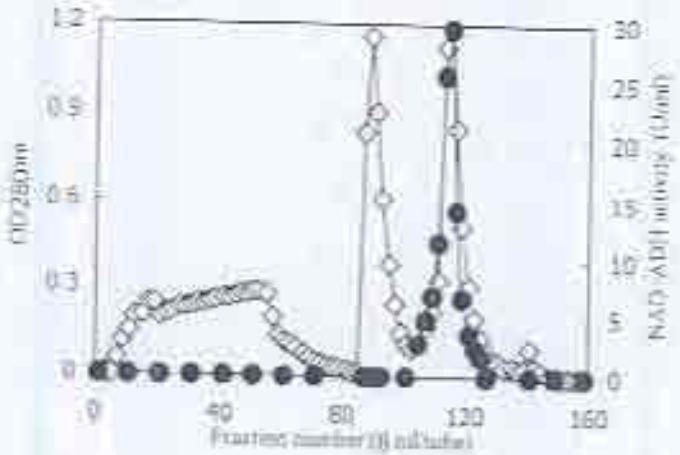

Figure 18 Elution pattern of NAD-dependent ADH II on hydroxyl apatite column chromatography. The combined active fraction from DEAE-Toyopearl column II (no. 11-43) contained 207 mg of protein was applied on a hydroxyl apatite column equilibrated with 50 mM KPB (pH 7.5). The protein was eluted step wise of 50, 100 and 500 mM KPB (pH 7.5). Each fraction (6 ml) was analyzed for protein (OD_{280}nm, —◇—) and NAD-ADH activity (—●—).

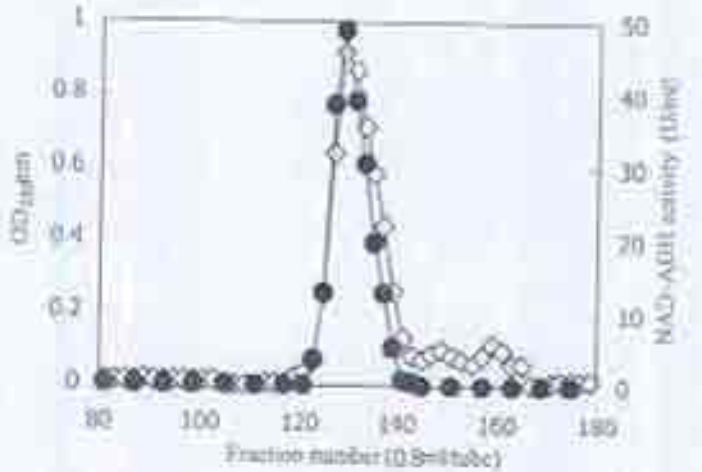

Figure 19 Elution pattern of NAD-dependent ADH II on Superdex S-200 column chromatography. The combined active fraction from hydroxyl apatite column (no. 105-125) contained 97.8 mg of protein was concentrated and 1.5 ml of the concentrated enzyme was applied on a Superdex S-200 column equilibrated with 50 mM KPB (pH 7.5). The protein was eluted with the same buffer. Each fraction (0.8 ml) was analyzed for protein (OD_{280}nm —◇—) and NAD-ADH activity (—●—).

Table 4 Summary of the purification of NAD-dependent ADHs (ADH I and ADH II) from the soluble fraction of *A. pasteurianus* CN5-2 NTG mutant strain.

Purification step	Total activity (U)	Total protein (mg)	Specific activity (U/mg)	Purification (fold)	Yield (%)
Crude extract[a]	37,100	1,830	16.7	1	100
DEAE-Toyopearl I[a]	17,400	822	20.9	1.2	96
ADH I[b]					
DEAE-Toyopearl II[a]	12,800	282	45.3	2.7	41
Hydroxyl apatite[a]	8,150	54.2	338	20	26
DEAE-Toyopearl III[a]	4,740	7.92	597	35	15
ADH II[b]					
DEAE-Toyopearl II[b]	9,000	207	43.0	2.6	20
Hydroxyl apatite[b]	7,820	92.8	84.3	5.0	25
Superdex S-200[b]	2,100	6.01	351	21	7.0

Note: [a]Activity was measured by the reduction of acetaldehyde at the final concentration of 10 mM, as described for the reverse reaction for ADH I in Materials and Methods.

[b]Activity was measured with 100 mM acetaldehyde as the substrate, as described for the reverse reaction for ADH II in Materials and Methods.

4.2 Purity and molecular mass determination

The purified enzyme fractions of ADH I and ADH II obtained from the final step, had a single protein band in SDS-PAGE (Figure 20 A and B). Moreover, the crystallization of ADH II was done and the grain shape of purified ADH II crystal was observed as shown in Figure 21. The relative molecular masses of ADH I and ADH II were estimated by SDS-PAGE to be 42 and 31 kDa, respectively. The native molecular sizes measured by a Superdex S-200 gel filtration were 130 and 70 kDa respectively, suggesting that the native ADH I is probably a trimer composed of identical subunits, while ADH II consists of two identical subunits.

Figure 20 SDS-PAGE of the purified ADH I and ADH II. (A) SDS-PAGE of the purified ADH I; Lane 1: crude extract (10 μg of protein), Lane 2: DEAE-Toyopearl I combined active fraction (10 μg), Lane 3: DEAE-Toyopearl II combined active fraction (10 μg), Lane 4: Hydroxyl apatite combined active fraction (10 μg), and Lane 5: DEAE-Toyopearl III combined active fraction (10 μg). (B) SDS-PAGE of the purified ADH II; Lane 1: crude extract (10 μg of protein), Lane 2: DEAE-Toyopearl I combined active fraction (10 μg), Lane 3: DEAE-Toyopearl II combined active fraction (10 μg), Lane 4: Hydroxyl apatite combined active fraction (10 μg), and Lane 5: Superdex S 200 combined active fraction (10 μg).

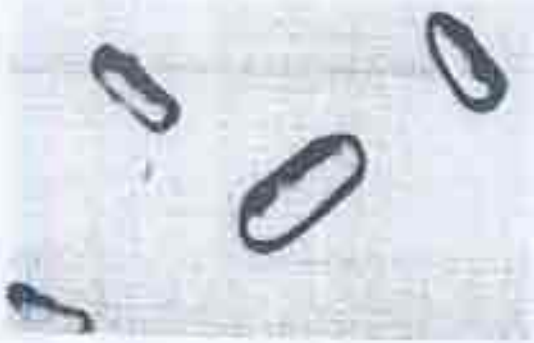

Figure 21 Crystals of NAD-dependent ADH II from *A. oosteruianus* Ch6-2 NTG mutant strain. The photomicrogram was taken under 200-fold of magnification.

4.3 N-terminal amino acid sequence analysis

The N-terminal amino acid sequence of ADH I (20 residues) and ADH II (30 residues) were serine-glycine-lysine-methionine-lysine-alanine-alanine-valine-valine-histidine-glutamic acid-phenylalanine-glycine-lysine-proline-leucine-threonine-isoleucine-glutamic acid-glutamic acid (SGKMKAAVVHEFGKPLTIEEI and alanine-arginine-valine-alanine-glycine-lysine-valine-alanine-isoleucine-valine-serine-glycine-alanine-alanine-asparagine-glycine-isoleucine-glycine-lysine-alanine-threonine-alanine-glutamine-leucine-leucine-alanine-lysine-glutamic acid-glycine-alanine (ARVAGKVAIVSG AANGIGKATAQLLAKEGA, respectively. In a database search using the BLAST algorithm, the ADH I sequence showed the best matching scores at the terminus of prokaryotic long-chain ADHs, especially from *Sinorhizobium meliloti* (NC_003037, Barnett *et al.*, 2001), *Ralstonia solanacearum* (AL646075, Salanoubat *et al.*, 2002), and *Pseudomonas aeruginosa* (AE004952, Stover *et al.*, 2000) as shown in Figure 22A. Based on the same procedures, ADH II was shown to have identity with short-chain ADHs, from *Agrobacterium tumefaciens* (AE008318, Hinkle *et al.*, unpublished), *Mycobacterium tuberculosis* (AE006970, Fleischmann *et al.*, unpublished), and *Caenorhabditis elegans* (AC006677, Waterston, 1998) as shown in Figure 22B. The data indicated that ADH I and ADH II belong to a long-chain and a short-chain ADH family, respectively.

A)

```
Long-chain alcohol dehydrogenase
NAD-ADH I
Sinorhizobium meliloti                          SGKMKAAVVHEFGKPLTIEE
Ralstonia solanacearum                            MIAAVVREYGKPVTIEE
Pseudomonas aeruginosa                            MKAAVVHAFGEPLRIED
                                  MKAAVVHAYGAPLEIE
                                                  * **** * *  **
```

B)

```
Short-chain alcohol dehydrogenase                    -GXXXGXG-
NAD-ADH II                    ARVAGKVAIVSGAANGIGKATAQLLAKEGA
Caenorhabditis elegans        GKVALVTGSSNGIGRATAVLLAQEGA
Mycobacterium tuberculosis                      KVAIVTGAAQGIGQAYAQALARKGA
Agrobacterium tumefaciens                     RLEGKVAIVTGAGRGIGRATAKLLATEGA
                                                *** * *  *** * *  ** ***
```

Figure 22 Alignment of the N-terminal amino acid sequence of NAD-dependent ADHs, ADH I (A) and ADH II (B) from *A. pasteurianus* GN6-2 NTG mutant strain. The consensus motif for NAD-binding is indicated above the alignment. GXXXGXG, glycine-rich consensus; *, highly conserved residues.

4.4 Kinetic properties of the purified enzymes

The apparent K_m and V_{max} values were measured for the two substrates, ethanol and acetaldehyde. Kinetic constants were also measured for the cofactors, NAD and NADH. These kinetic data were summarized in Table 5. K_m values of ADH I for ethanol and acetaldehyde were lower than those of ADH II. From the values of both K_m and V_{max}, both enzymes were clearly suggested to operate with a bias toward the reduction of acetaldehyde to ethanol. Of these kinetic constants in both enzymes, only ADH I had substrate inhibition against acetaldehyde at the higher concentration over 10 mM, where the K_i value was estimated to be 57.3 mM (data not shown). However, since both ADH I and ADH II are induced 17 and 20 times, respectively, when the NTG mutant strain was grown in the medium containing ethanol.

As for the ethanol oxidation, ADH I is more favorable than ADH II because ADH I has a lower K_m value and higher V_{max} for ethanol than ADH II. However, since the K_m value of ADH II for acetaldehyde was very high, 24 mM, compared with that of ADH I, the reverse reaction was relatively unlikely to occur at low levels of acetaldehyde. Thus, ADH II may work for ethanol oxidation to acetaldehyde even when acetaldehyde was accumulated at some level. This notion may be supported by the finding that K_m values for NAD and NADH of ADH II, especially for NAD, were extremely low compared with those of ADH I. Thus, ADH II seemed to be mainly involved in ethanol assimilation under the conditions that the NAD level was low and acetaldehyde was relatively high, which may occur at the second stage when *A. pasteurianus* CN6-2 NTG mutant strain grown on ethanol medium. In contrast, ADH I seemed to work for ethanol assimilation at the initial stage of the cell growth in the presence of ethanol, where ethanol concentration of the cell was high enough but that of acetaldehyde was marginal. Both ADH I and ADH II were NAD-specific and totally inactive when NADP was used as coenzyme.

Table 5 Kinetic constants of NAD-dependent ADHs from *A. pasteurianus* CN6-2 NTG mutant strain

Substrate or cofactor	ADH I		ADH II	
	K_m (mM)	V_{max} (U/mg)	K_m (mM)	V_{max} (U/mg)
Ethanol	2.9	9.0	7.3	0.04
Acetaldehyde	0.3	375	24	222
NAD	1.2	55.6	0.04	0.05
NADH	0.2	500	0.03	90

Kinetic constants for ethanol were measured with various concentrations of ethanol and 0.1 mM NAD as described in Materials and Methods (the forward reaction), while that for acetaldehyde was done with various concentrations of acetaldehyde and with 0.1 mM NADH as described as the reverse reaction for ADH I or for ADH II in Materials and Methods. Kinetic constants for NAD was done with various concentrations of NAD and 100 mM ethanol, while that for NADH with various concentrations of NADH and 100 mM acetaldehyde, as described as the forward and reverse reactions, respectively.

4.5 Substrate specificity of the purified enzymes

Substrate specificity of crude extract, NAD-dependent ADH I and ADH II were shown in Table 6. The crude extracts of *A. pasteurianus* GN6-2 NTG mutant strain grown on ethanol contained NAD-dependent ADHs active on the reduction of wide range of aldehydes, and also on the oxidation of primary, secondary, and cyclic alcohols. The purified ADH I showed a broad substrate specificity for primary alcohols (C_2 to C_6), cyclobutanol, benzylalcohol, and several aldehydes. Acetaldehyde or propionaldehyde as a substrate for the reverse reaction was the most suitable substrate tested. In contrast, the purified ADH II showed a preference for secondary alcohols and aldehydes, and butylaldehyde was the best substrate tested. Cyclic alcohols were also oxidized with ADH II, but at a lower rate. Of the secondary alcohols, activity against stereoisomers of 2-butanol, 2-hexanol, and 2-octanol was also examined with ADH II. As shown in Table 6, the enzyme appears to be highly specific for the *R*-(-)-stereoisomer and shows the enantioselectivity for the R isomer, *R*-(-)-2-butanol, R-(-)-2-hexanol, and R-(-)-2-octanol, respectively, for 2-butanol, 2-hexanol, and 2-octanol.

The substrate specificity of ADH I is similar to almost all of the known long-chain ADH family from yeast and other microorganisms (Dickinson and Dalziel, 1967; Dalziel and Dickinson, 1966; Azoulay and Heyderman, 1963; Tassin and Vandecasteele, 1972). In contrast, ADH II is rather unique in showing a preference for long-chain secondary alcohols such as R-(-)-2-hexanol or *R*-(-)-2-octanol, which is very rare case in the secondary alcohol-specific ADHs so far described. The other ADHs in this family that have a preference for secondary alcohols showed the optimal activity with 2-propanol or 2-butanol and have rather poor activity with long-chain secondary alcohols greater than 2-hexanol (Bryant et al., 1968; Coleman and Perry, 1985; Hou *et al.*, 1979; Patel et al., 1978; Schutte et al., 1982). However, the selectivity for R-(-)-

stereoisomers of ADH II is similar to almost all short-chain ADHs known. ADHs reacting with secondary alcohol are obtained from methylotrophic bacteria or yeast (Hou et al., 1981; Barnett et al., 1980; Hou et al., 1983). *Comamonas terrigena* prefers preferentially the R-(-)-stereoisomer (Barnett et al., 1981), whereas *Rhodococcus erythropolis* enzyme is specific for the S-(+) stereoisomer (Ludwig et al., 1998). Interestingly, there is no report on NAD-dependent ADHs with an extremely high specific activity towards long-chain secondary alcohols (C_8-C_{12}).

Table 6 Substrate specificity of NAD-dependent ADHs in crude extract, ADH I and ADH II of *A. pasteurianus* CNS-2 N1G mutant strain

Substrate (10 mM)	Crude extract		ADH I		ADH II	
	U/mg	(%)*	U/mg	(%)*	U/mg	(%)*
Primary alcohol						
Ethanol	0.078	(100)	16.4	(100)	0.20	(<1)
1-Propanol	0.75	(96)	14.7	(90)	0.38	(<1)
1-Butanol	0.83	(106)	13.4	(82)	1.30	(<1)
1-Pentanol	0.07	(9)	2.42	(15)	0.34	(<1)
1-Hexanol	0.70	(90)	5.78	(35)	3.21	(2)
1-Heptanol	0.45	(58)	8.55	(52)	0.82	(<1)
1-Octanol	0.22	(28)	1.86	(11)	0.38	(<1)
1-Nonanol	0.14	(18)	2.97	(18)	0.34	(<1)
1-Decanol	0.07	(9)	3.16	(19)	0	(0)
Secondary alcohol						
2-Propanol	0.91	(117)	2.60	(16)	22.9	(12)
2-Butanol	1.71	(219)	1.67	(10)	84.2	(46)
S-(+) 2-Butanol	0.56	(72)	1.30	(8)	18.4	(10)
R-(-)-2-Butanol	2.66	(341)	0.37	(2)	107	(58)
2-Pentanol	2.46	(315)	0	(0)	68.9	(37)
2-Hexanol	4.69	(601)	0	(0)	168	(91)
S-(+)-2-Hexanol	0.42	(54)	0	(0)	9.95	(5)
R-(-)-2-Hexanol	4.59	(601)	0	(0)	184	(100)
2-Octanol	4.37	(560)	0	(0)	153	(83)
S-(+)-2-Octanol	0.10	(13)	0	(0)	2.30	(1)
R-(-) 2-Octanol	3.05	(392)	0	(0)	138	(75)

Table 6 (Continued)

Substrate (10 mM)	Crude extract U/mg	(%)[a]	ADH I U/mg	(%)[a]	ADH II U/mg	(%)[b]
Cyclic alcohol						
Cyclobutanol	0.93	(119)	11.9	(73)	8.73	(5)
Cyclopentanol	0.02	(3)	0	(0)	0.23	(<1)
Cyclohexanol	0.36	(46)	0	(0)	13.0	(7)
Cyclooctanol	0.32	(41)	0	(0)	6.43	(4)
Benzylalcohol	0.25	(32)	1.78	(0)	0	(0)
Aldehyde						
Formaldehyde	0.07	(9)	2.23	(14)	0.92	(<1)
Acetaldehyde	19.5	(2500)	364	(2219)	337	(183)[c]
Propionaldehyde	19.9	(2561)	223	(1380)	551	(299)
Butylaldehyde	35.4	(4282)	96.6	(589)	868	(483)
Valeraldehyde	2.78	(356)	20.4	(124)	7.04	(4)
Anisaldehyde	2.91	(261)	4.28	(26)	2.79	(2)

Note: Activities for primary, secondary, and cyclic alcohols were measured by the forward reaction, while those for aldehydes, by the reverse reaction, as described in Materials and Methods.

[a]The activity with ethanol of the crude extract and of ADH I were defined as 100%.

[b]The activity with *R*-(-)-2-Hexanol of ADH II was defined as 100%.

[c]Measured with 100 mM acetaldehyde at the final concentration.

4.6 Metal content and effects of metal ions on the enzyme activity

Metal content of the NAD-dependent ADHs dialyzed against 20 mM 2-[4-(2-Hydroxyethyl)-1-piperazinyl] ethanesulfonic acid (HEPES) buffer (pH 7.5) in the absence or presence of EDTA were shown in Table 7. Metal analyses revealed the presence of 1.225 and 0.995 mol of Zn^{2+} per mol of ADH I subunit in the absence and presence of EDTA, respectively. The data suggested that each subunit of ADH I contained 1 mole of Zn^{2+}, but ADH II seemed not to contain any specific metal, at least after dialysis. Consequently, native ADH I contained 3 Zn^{2+} atoms per molecule. The effects of metal ions and EDTA on the activity of NAD-dependent ADHs were also studied. The Zn^{2+} seemed to be tightly bound in the active site of the enzyme,

since EDTA treatment did not remove the metal from the enzyme. This situation of ADH I was similar to other long-chain ADH family such as ADH from propane-grown *Pseudomonas fluorescens* NRRLB-1244 (Hou *et al.*, 1983), and NAD-dependent ADH of thermoacidophilic archaebacterium (Ammendola *et al.*, 1992), where Zn^{2+} in the enzyme was stable against EDTA treatment. Although ADH II seems not to contain any significant level of Zn^{2+} or Mg^{2+}, the enzyme activity was accessed by EDTA treatment but recovered by Mg^{2+} treatment. In addition, ADH II activity could be stabilized by the addition of 1 mM $MgCl_2$ in the column buffer during the purification. Thus, Mg^{2+} seemed to work for maintaining the enzyme stable and active.

Table 7 Metal content in NAD-dependent ADHs from *A. pasteurianus* CN6-2 NTG mutant strain

Enzyme	EDTA[a] (μM/μM enzyme)			-EDTA[b] (μM/μM enzyme)		
	Zn^{2+}	Mg^{2+}	Fe^{2+}	Zn^{2+}	Mg^{2+}	Fe^{2+}
ADH I	1.205	0.080	0.035	0.995	0.145	0.035
ADH II	0.079	0.061	0.020	0.150	0.123	0.020

Note: [a]Both ADHs were dialyzed against 20 mM HEPES buffer at pH 7.5 in the absence of EDTA.

[b]Both ADHs were dialyzed against 20 mM HEPES buffer at pH 7.5 in the presence of 5 mM EDTA.

All of the characterization of NAD-dependent ADHs (ADH I and ADH II) were summarized in Table 8. In conclusion, two NAD-ADHs (ADH I and ADH II) induced by ethanol in *A. pasteurianus* CN6-2 NTG mutant strain were purified from the soluble fraction. ADH I is a trimer enzyme with molecular mass of 130 kDa consisting of 3 subunits (42 kDa for each subunit). Each subunit contained 1 mole of Zn^{2+}. Its substrate specificity was similar to almost all of known long-chain ADH family. By contrast, ADH II is a dimmer enzyme with molecular mass of 70 kDa consisting of 2 subunits (31 kDa for each subunit). Both ADH I and ADH II possessed some similar characteristics i.e. optimum pH for ethanol oxidation, pH stability and thermostability. The obvious different properties of those two NAD-ADHs were kinetic constants (K_m and V_{max}) for ethanol oxidation, acetaldehyde reduction, NAD and NADH. In addition, both of them showed different substrate specificity.

Table 8 Summary of characteristics of NAD-dependent ADHs (ADH I and ADH II)

Characteristics	ADH I	ADH II
Molecular mass (SDS-PAGE)	42 kDa	31 kDa
Native enzyme (Superdex S-200 gel filtration)	130 kDa	70 kDa
Subunit	Tetrameric enzyme	Dimeric enzyme
Optimum pH for ethanol oxidation	9.5	8.5
Optimum pH for acetaldehyde reduction	6.5	6.0
pH stability for ethanol oxidation	5.5-8.0	5.5-8.0
pH stability for acetaldehyde reduction	5.0-8.5	5.0-8.5
Thermostability for ethanol oxidation	65°C	65°C
Thermostability for acetaldehyde reduction	70°C	65°C
K_m for ethanol oxidation	2.3 mM	7.3 mM
V_{max} for ethanol oxidation	9.0 U/mg	0.04 U/mg
K_m for acetaldehyde reduction	0.3 mM	24 mM
V_{max} for acetaldehyde reduction	375 U/mg	222 U/mg
K_m for NAD	1.2 mM	0.04 mM
V_{max} for NAD	55.9 U/mg	0.05 U/mg
K_m for NADH	0.2 mM	0.03 mM
V_{max} for NADH	500 U/mg	90 U/mg
Metal content	Zn^{2+} sufficient	No metal
Substrate specificity for oxidation reaction	Ethanol	R-(-)-2-Hexanol
Substrate specificity for reduction reaction	Acetaldehyde	Butyraldehyde

5. Construction of *adhA* gene disruptant

ADH-disruptant was constructed by homologous recombination using kanamycin gene disruption cassette as described in Materials and Methods. The schematic diagram for construction of ADH-disuptant is shown in Figure 23. The kanamycin resistant transformants were selected on YPG medium containing 50 μg/ml of kanamycin, 0.5% $CaCO_3$ and 2% ethanol. Colonies deficient in ethanol-oxidizing ability were screened by the absence of clear zone. The model of homologous recombination was shown in Figure 24A. The transformants were isolated and confirmed by PCR amplification, compared with wild strain. The PCR product from ADH-disruptant DP3 (3.1 kb) showed 1.2 kb larger than wild strain (1.9 kb), which corresponded to the insertion of the kanamycin cassette (Figure 24B). Thus, characterization of ADH-disruptant

DP3 and NTG mutant CN8-2 strains as described above were done and compared with wild strain, to elucidate the function of cofactor-free ADH.

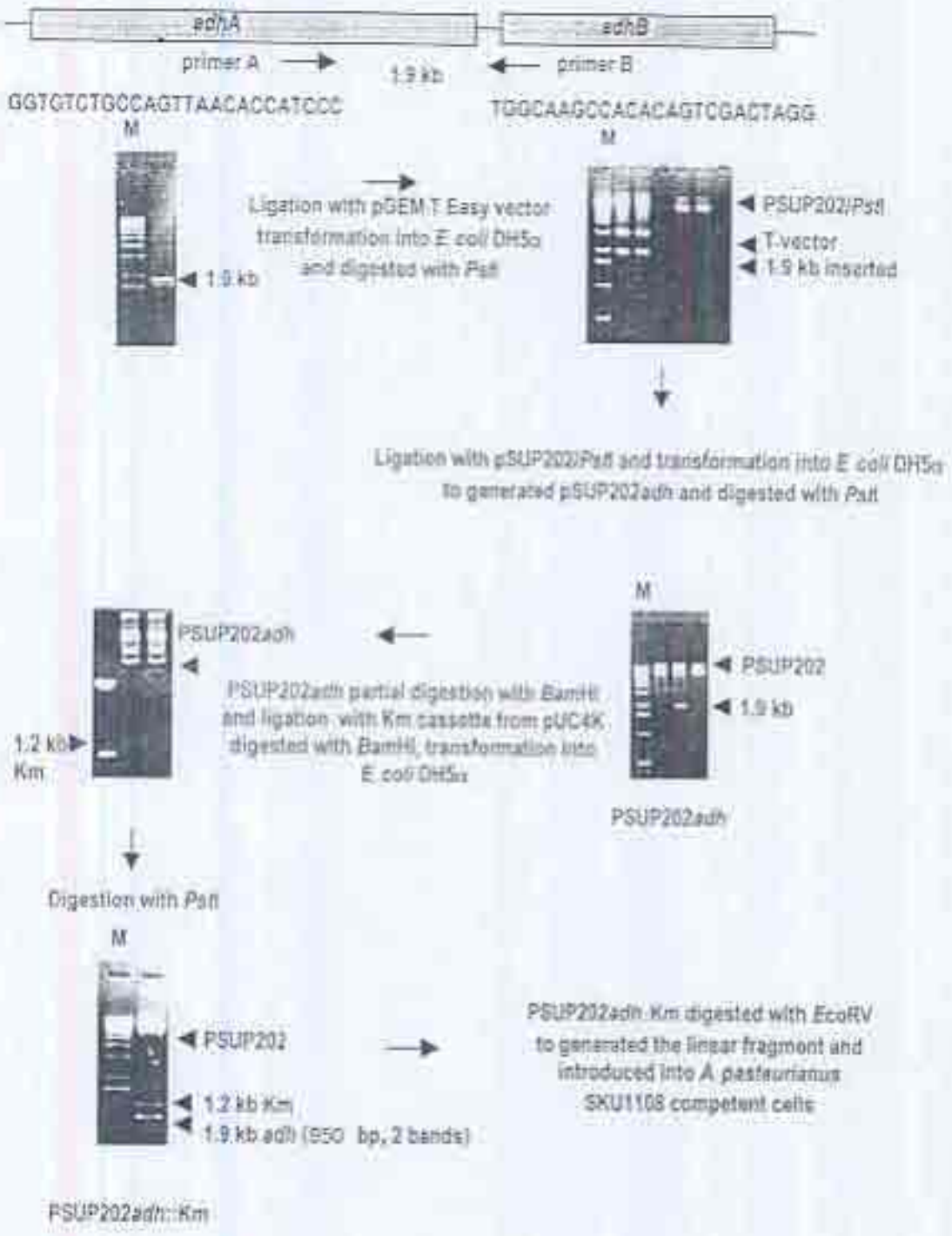

Figure 23 Schematic diagram for construction of ADH disruptant from *A. pasteurianus* SKU1108.

A)

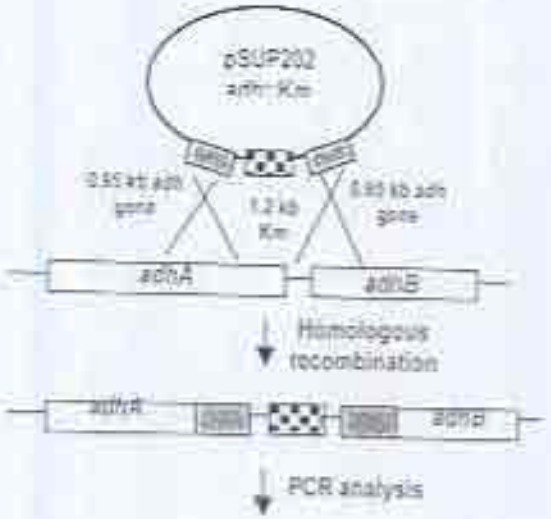

B)

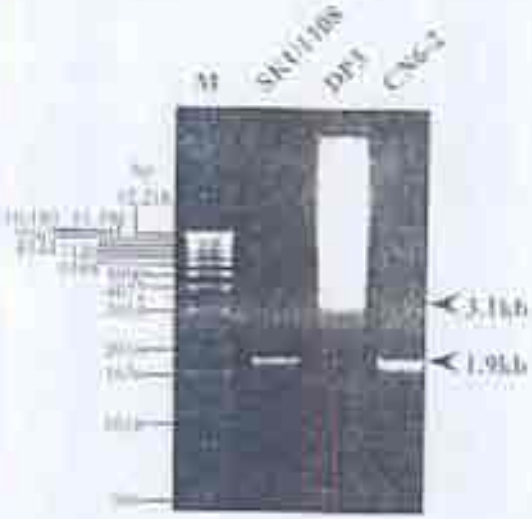

Figure 24 Agarose gel electrophoresis of PCR product obtained from *A. pasteurianus* SKU1108, disruptant DP3 and NTG mutant CN6-2. PCR was carried out by using the primer A and B.

6. Comparison of physiological characteristics between *A. pasteurianus* SKU1108, NTG mutant CN6-2 and ADH-disruptant DP3

5.1 Comparison of enzyme activities involved in ethanol oxidation

The ethanol-oxidizing ability of *A. pasteurianus* SKU1108, disruptant DP3 and NTG mutant CN6-2 were compared on YPGD medium supplemented with 2% ethanol and 0.5% $CaCO_3$ (Figure 25). ADH-deficient strain CN6-2 could not produce any clear zone, while ADH disruptant strain DP3 produce a small clear zone when compared with wild strain.

Figure 25 Comparison of clear zone formation of disruptant DP3 and NTG mutant CN6-2 with *A. pasteurianus* SKU1108. These strains were spotted on YPGD medium containing 0.5% $CaCO_3$ and 2% ethanol and incubated for 24 h at 30°C.

To quantitatively analysis these mutations, the enzyme activities involved in ethanol oxidation were assayed in both membrane and soluble fractions as shown in Table 9. In the wild-type strain, both membrane-bound ADH and ALDH activities were induced by the addition of ethanol into the culture medium, while cytoplasmic NAD-dependent ADH activity was kept lowér. This situation was similar to the case of *A. pasteurianus* NCI1380 in which ADH activity was enhanced more than 10-fold by ethanol (Takemura et al., 1993). In both DP3 and CN6-2 strains, both membrane-bound ADH and ALDH were dramatically decreased, which is more complete in CN6-2 strain. Ethanol and acetaldehyde oxidase activities were also changed parallel to the change of the dehydrogenase activities. The decrease in ALDH and aldehyde oxidase activities were not so intensive in DP3 strain compared to CN6-2 strain. Contrary to the membrane-bound ADH activity, NAD-dependent ADH activity was increased in both mutants DP3 and CN6-2, in which CN6-2 strain showed higher activity than DP3 strain in the reverse